

### 30. MAESTRICHTIAN CALCAREOUS NANNOFOSSIL BIOSTRATIGRAPHY OF MAUD RISE ODP LEG 113 SITES 689 AND 690, WEDDELL SEA<sup>1</sup>

James J. Pospichal<sup>2</sup> and Sherwood W. Wise, Jr.<sup>2</sup>

#### ABSTRACT

Recovery of an essentially complete upper Maestrichtian/lower Paleocene interval on Maud Rise at 65°S latitude in the Weddell Sea during Ocean Drilling Program Leg 113 marks the first time that this interval has been cored at these high latitudes. The entire interval was missing at all Falkland Plateau sites drilled during DSDP Legs 36 and 71. Maestrichtian nannofossil assemblages in sediments from Sites 689 and 690, therefore, provide the basis for a needed revision of Maestrichtian coccolith zonation schemes for high southern latitudes. Three zones and two new subzones are described: the uppermost Maestrichtian *Nephrolithus frequens* Zone, which is subdivided into the *Cribrosphaerella daniae* Subzone and the underlying *N. corystus* Subzone, and the *Biscutum magnum* and *B. coronum* Zones.

A complete calcareous nannofossil biostratigraphy based on the proposed scheme is given including a description of individual species abundance, preservation, and stratigraphic distribution. At this site, the southernmost carbonate site yet drilled by DSDP/ODP, it is evident that the Falkland Plateau Nannofossil Biogeographic Province can be extended to the margins of Antarctica. In addition, the biogeographic ranges of many calcareous nannofossils can likewise be extended. Last, we hypothesize that *Nephrolithus frequens* evolved from *N. corystus* prior to its dispersal to the lower latitudes where it is an important zonal marker.

Three new taxa, *Neocrepidolithus watkinsii* n. sp., *Nephrolithus frequens miniporus* emend. n. comb, and *Psyktosphaera firthii* n. gen., n. sp. are described.

#### INTRODUCTION

During ODP Leg 113, drilling took place at nine sites in the Weddell Sea of the Atlantic sector of the Southern Ocean (Fig. 1). Sites 689 and 690, located on Maud Rise, 700 km off East Antarctica, contain a Cenozoic to upper Mesozoic calcareous-siliceous biogenic sequence beneath the present day Antarctic water mass. The cores were used to study relationships between Antarctic paleoceanographic development and changes in calcium carbonate and siliceous biogenic sediments. Site 689 lies approximately 116 km northeast of Site 690, which is down-slope on the southwest flank of Maud Rise as shown in the bathymetric profile in Figure 2. Basement rocks of Maud Rise are ocean island basalts derived from hot spot volcanism, and are of presumed Cenomanian age (Shipboard Scientific Party, 1988a, p. 184, 198–202).

All samples of calcareous sediments from both sites yielded abundant calcareous nannofossils. Coccoliths are generally poorly to moderately well-preserved with good preservation noted in only a few intervals. A calcareous nannofossil biostratigraphy of Maestrichtian sediments from Sites 689 and 690, which includes two new subzones, is presented in this study. Individual species abundance and preservation data are shown in Tables 1 and 2.

This is the first upper Maestrichtian-lower Paleocene interval recovered in the Atlantic sector of the Southern Ocean by deep sea drilling. Previous drilling by DSDP Legs 36 (Barker, Dalziel, et al., 1977) and Leg 71 (Ludwig, Krashennikov, et al., 1983) on the Falkland Plateau revealed a discontinuous sedimentary sequence through the Campanian-lower Maestrichtian and upper Paleocene, which provided the initial data for Southern Ocean calcareous nannofossil biostratigraphic schemes for this interval by Wise and Wind (1977), Wind (1979a), and Wind and

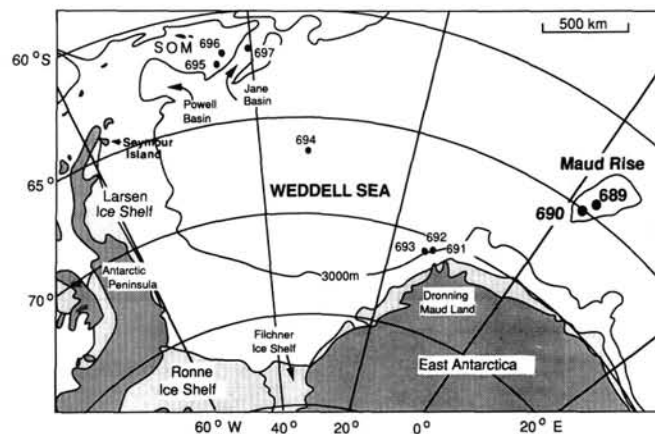


Figure 1. Location map of Sites 689, 690, and other ODP Leg 113 Sites, Weddell Sea off East Antarctica. SOM = South Orkney microcontinent.

Wise (1983). With the addition of the new material from ODP Sites 689 and 690, we propose an emended version of the previously proposed high southern latitude schemes. In addition, we confirm the extension of the Falkland Plateau Biogeographic Province of Wind (1979b) to the margins of East Antarctica. Last, we document the high latitude transition of *Nephrolithus corystus* to *N. frequens*, apparently prior to the dispersal of the latter to lower latitudes where it is recognized as an important zonal marker.

#### METHODS

Smear slides of raw sediment were examined at  $\times 1000$  using the light microscope in order to estimate relative calcareous nannofossil abundance, preservation, and relative abundance of individual species. The JEOL 840 scanning electron microscope (SEM) was employed to aid in precise identification of species and description of new taxa.

<sup>1</sup> Barker, F. P., Kennett, J. P., et al., 1990. *Proc. ODP, Sci. Results*, 113: College Station, TX (Ocean Drilling Program).

<sup>2</sup> Department of Geology, Florida State University, Tallahassee, FL 32306.

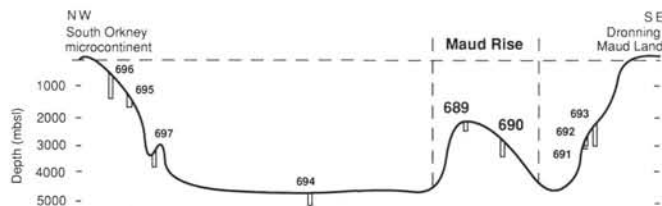


Figure 2. Bathymetric profile of Maud Rise projected to the west (see Fig. 1) along a schematic northwest-southeast transect across the Weddell Sea, showing the relative positions and depth distributions of the Leg 113 sites. mbsl = meters below sea level.

Estimates of overall nannofossil abundance were given the following letter codes: V = very abundant (>10 nannofossils/field of view); A = abundant (1-10 nannofossils/field of view); C = common (at least 1 nannofossil/2 fields of view); F = few (<1 nannofossil/2 fields of view).

Average state of preservation of nannofossils per sample is designated in the following way: G = good (little or no etching or overgrowth); M = moderate (some etching and/or overgrowth, identification of species is typically not impaired); P = poor (strong etching and/or overgrowth, identification of species is impaired but often still possible).

Relative individual species abundance estimates follow the procedure of Hay (1970) and are indicated in the following manner: V = very abundant (>10 specimens/field of view); A = abundant (1-10 specimens/field of view); C = common (1 specimen/2-10 fields of view); F = few (1 specimen/11-100 fields of view); R = rare (1 specimen/101-1000 fields of view); P = present (only 1 specimen observed/slide).

Taxa considered in this report are listed in the Appendix. Bibliographic references for these species are given in Loeblich and Tappan (1966-1973), van Heck (1979-1983), and Steinmetz (1984a-1989). Any taxa not cited therein are given in the references.

**BIOSTRATIGRAPHIC ZONATION**

Commonly used comprehensive calcareous nannofossil zonation schemes have been compiled for the Cretaceous by Sissingh (1977), Roth (1978), and Perch-Nielsen (1979a) (see Perch-Nielsen, 1985, for summary). The schemes have been developed mostly from low latitude sections or northern high latitude sequences and, until recently, have had little chance to be tested in southern high latitudes. Deep sea drilling on the Falkland Plateau in the South Atlantic during DSDP Legs 36 and 71 recovered a discontinuous sequence through the Campanian and Maestrichtian. As previously mentioned, a distinct high latitude provincial nannoflora was described from these sections by Wise and Wind (1977), Wind (1979a, b), and Wise (1983). From this material, Wind (1979a) was able to develop a calcareous nannofossil zonation for the Campanian-Maestrichtian of the Southern Oceans. However, the sequences Wind based his scheme on were either not continuously cored or contained missing sections; thus many uncertainties remained. An amendment was later proposed by Wise (1983) for the definition of Wind's upper Campanian/lower Maestrichtian *Biscutum coronum* Zone, and Wind and Wise (1983) cross-correlated that scheme with Sissingh's zonation. The current status of the high latitude zonations is reviewed by Wise (1988).

With the recovery of the material from Maud Rise, gaps in the middle and upper Maestrichtian left by coring during DSDP Legs 36 and 71 can be filled. An updated coccolith zonation is described below and shown in Figure 3 with correlations to zonation schemes of Sissingh (1977) and Roth (1978).

AGE		Sissingh (1977)	Roth (1978)	This Paper	
Maestrichtian	late	<i>N. frequens</i> (CC26)	<i>M. murus</i> (NC23)	<i>N. frequens</i>	<i>C. daniae</i>
		<i>A. cymbiformis</i> (CC25)	<i>L. quadratus</i> (NC22)		
	early	<i>R. levis</i> (CC24)	<i>L. praequadratus</i> (NC21)	<i>N. corystus</i>	<i>B. magnum</i>
		<i>T. phacelosus</i> (CC23)	<i>T. trifidus</i> (NC20)		
Campanian				<i>B. coronum</i>	

Figure 3. Maestrichtian biostratigraphic zonation of this report correlated with Sissingh (1977) and Roth (1978).

*Nephrolithus frequens* Zone

**Definition.** The interval from the last occurrence (LO) of *Biscutum magnum* to the Cretaceous/Tertiary boundary, which in this region is best approximated by the first occurrence (FO) of *Biantholithus sparsus* (see comment below).

**Age.** Late Maestrichtian.

**Authors.** Cepék and Hay (1969), modified as a high latitude provincial zone in this paper.

**Associated species.** *Acuturris scotus*, *Arkhangelskiella cymbiformis*, *A. specillata*, *Cribrosphaerella daniae*, *Kampferius magnificus*, *N. corystus*, *Prediscosphaera cretacea*, *P. stoveri*, *Zygodiscus spiralis*, *Nephrolithus frequens miniporus* emend., n. comb.

**Comments.** The LO *Reinhardtites levis* or the FO of *N. frequens* may be used to approximate the base of this zone; however, where preservation is not ideal *N. frequens* may not be distinguished from *N. corystus*. As suggested by Worsley (1974), *N. frequens* is apparently time-transgressive toward the lower latitudes (see Discussion section).

Perch-Nielsen (1979a) suggested the use of the FO of *Biantholithus sparsus* to mark the top of the zone, which in this region would be the most appropriate nannofossil to denote Tertiary strata. In Hole 690C, however, the K/T boundary section is complicated by intense bioturbation, and the boundary is placed at the top of the last remaining relict Cretaceous ooze/chalk (Pospichal and Wise, this volume, chapter 32).

*Cribrosphaerella daniae* Subzone

**Definition.** Interval from the LO of *Nephrolithus corystus* to the Cretaceous/Tertiary boundary (see above discussion).

**Age.** Late Maestrichtian.

**Reference Section.** ODP Hole 690C, 247.81-277.76 mbsf, Maud Rise.

**Associated species.** As above less *N. corystus*.

**Comments.** A *C. daniae* Zone was proposed by Wind (1979a) for the interval corresponding to the *N. frequens* Zone presented here. The zonal name is retained here for the subzone as the species, *C. daniae*, is quite persistent throughout this interval.

*Nephrolithus corystus* Subzone

**Definition.** Interval from the LO of *B. magnum* to the LO of *N. corystus*.

**Age.** Late Maestrichtian.

**Reference Section.** ODP Hole 690C, 274.17–277.76 mbsf, Maud Rise.

**Associated species.** As above plus *N. corystus*.

**Comments.** Due to a disconformity, the interval containing the overlap of *N. frequens* and *N. corystus*, which occurs near the base of the *N. frequens* Zone was not cored on the Falkland Plateau. The overlap was first noted by Wind (1979a) at DSDP Site 249 off South Africa and later by Harwood (in Huber et al., 1983) in sediments from Seymour Island, Antarctica. The overlap occurs for a very short interval at both Sites 689 and 690 (Tables 1, 2). As noted previously, the LO of *Reinhardtites levis* or the FO of *N. frequens* may serve as alternate markers for the base of this subzone.

*Biscutum magnum* Zone

**Definition.** The interval from the LO of *Biscutum coronum* to the LO of *B. magnum*.

**Author.** Wind (1979a, b).

**Age.** Middle Maestrichtian.

**Associated species.** In addition to those species mentioned above, *Zygodiscus compactus*, *Reinhardtites levis*, *B. dissimilis*, *B. notaculum*, *Lucianorhabdus cayeuxii*, *Centosphaera barbata*, *Monomarginatus quaternarius*, *Teichorhabdus ethmos*, *Psyktosphaera firthii* n. gen., n. sp., and *Neocrepidolithus watkinsii* n. sp.

**Comments.** As noted above, the FO of *N. frequens* was also noted to correspond closely to the LO of *B. magnum* at both Sites 689 and 690. In addition, the lack of a gap between the LO of *R. levis*, the last surviving species of *Reinhardtites*, and the FO of *N. frequens* is noted. This gap defines Sissingh's (1977) *Arkhangelskiella cymbiformis* Zone (CC25) (see Discussion section).

*Biscutum coronum* Zone

**Definition.** The interval from the LO of *Marthasterites furcatus* to the LO of *B. coronum*.

**Authors.** Wind (1979a), emended by Wise (1983).

**Age.** Early Campanian-early Maestrichtian.

**Associated species.** In addition to those mentioned above, *Vekshinella* sp., *Misceomarginatus pleniporus*, *Monomarginatus pectinatus*, *Tranolithus phacelosus*, *Biscutum constans*, and *Aspidolithus parvus*.

**Comments.** The original zone of Wind (1979a) was emended by Wise (1983), who gives a detailed discussion of the definition. Species such as *Aspidolithus parvus*, *Reinhardtites anthophorus*, *Tranolithus phacelosus*, and *Eiffellithus eximius* all have LO's near the Campanian/Maestrichtian boundary, and may be used to further subdivide and delimit the *B. coronum* Zone. A division of this interval based on these forms has not been proposed here due to the lack of a suitable section, as the Campanian portion of the interval was not cored on Maud Rise.

## SITE SUMMARIES

## Site 689 (Hole 689B, 64°31.01'S; 03°05.99'E)

Hole 689B was cored to a depth of 297.3 mbsf where persistent chert layers forced termination of drilling at ~30 m above basement. The Neogene section consists mostly of diatom ooze with interbeds of nannofossil ooze in the lower Miocene sequence and chert near the top of the Pliocene section. Calcareous nannofossil ooze and foraminifer-nannofossil ooze comprise the Oligocene to upper Paleocene unit, and foraminifer-nannofossil chalks with interbedded chert layers near the base make up the upper Paleocene to Maestrichtian sequence. Calcareous nannofossils are common to very abundant in the Maestrichtian cores, but preservation is generally poor. A complete list of species preservation and abundance for Hole 689B is given in Table 1. A summary of the nannofossil biostratigraphy and the magnetostratigraphy of Hamilton (this volume) is provided in Figure 4.

The sediments from the Cretaceous/Tertiary boundary in Sample 113-689B-25X-5, 83–84 cm (233.43 mbsf) (see Pospichal

and Wise, this volume, chapter 32) down to Sample 113-689B-28X-1, 29–31 cm (255.90 mbsf) are assigned to the *Nephrolithus frequens* Zone (Fig. 4). *N. frequens*, *Acuturris scotus*, *Arkhangelskiella cymbiformis/specillata*, *Cribrosphaerella daniae*, *C. ehrenbergii*, *Kamptnerius magnificus*, and *Prediscosphaera stoveri* are common to abundant through this interval. Also present are few *Ahmuelerella octoradiata*, *Zygodiscus spiralis*, *Markalius inversus*, *Micula decussata*, *Teichorhabdus ethmos*, and *Nephrolithus frequens minimiporus* emend., n. comb. At the base of this zone, in Section 113-689B-27X, CC (255.60 mbsf) and Sample 113-689B-28X-1, 29–31 cm (255.90 mbsf), rare to few *N. corystus* overlap with common *N. frequens*. This short interval is thus assigned to the *N. corystus* Subzone (Fig. 4). The interval above this lacks *N. corystus* and belongs to the *Cribrosphaerella daniae* Subzone.

Sediments of Samples 113-689B-28X-1, 135–137 cm (256.96 mbsf) to -29X-2, 28–30 cm (266.98 mbsf) are assigned to the *Biscutum magnum* Zone (Fig. 4). The interval is characterized by common *N. corystus*, *B. magnum*, *R. levis*, and *Z. compactus*. The use of the LO of *B. magnum* to mark the *N. frequens*/*B. magnum* Zone boundary is illustrated in Sample 113-689B-28X-1, 135–137 cm, where the last common occurrence of *B. magnum* precedes the first common *N. frequens* by one sample (Table 1).

Sediments of Samples 113-689B-29X-2, 130–132 cm (268.0 mbsf) to Section 113-689B-33X, CC (297.3 mbsf) assigned to the *Biscutum coronum* Zone contain a similar assemblage with the addition of rare to few *B. coronum*, *Neocrepidolithus watkinsii* n. sp., *Psyktosphaera firthii* n. gen., n. sp., and *C. surirellus*. Because of the absence of species such as *Aspidolithus parvus*, *Eiffellithus eximius*, and *R. anthophorus*, which are normally found in uppermost Campanian sediments, the interval is assigned to the lower Maestrichtian part of the *B. coronum* Zone (Fig. 4). *Tranolithus phacelosus*, a lower Maestrichtian zonal marker in Sissingh's (1977) scheme, is present in this zone but its occurrence is sporadic.

Nannofossil assemblages of Cores 113-689B-30X through -33X are dominated by the holococcolith, *Acuturris scotus* (Pl. 9, Figs. 6, 11). Although preservation is poor, the forms can be identified by their distinctive needle shape and high birefringence in the light microscope. Another holococcolith genus, *Lucianorhabdus* (Pl. 9, Figs. 7, 9–11) is also present but is not as abundant.

## Site 690 (Hole 690C, 65°09.63'S; 01°12.30'E)

Site 690, on the southwestern flank of Maud Rise, is located only 116 km southwest of Site 689. Hole 690C was drilled to basement at 317.0 mbsf with lithologies similar to those of Site 689 except for less chert and the presence of varying amounts of terrigenous sediment in the Maestrichtian-Paleocene units. Calcareous nannofossils are abundant in all samples examined, and preservation is markedly improved from Site 689. Table 2 provides a complete listing of species abundance and preservation for Hole 690C. The nannofossil biostratigraphy correlated with the magnetostratigraphy of Hamilton (this volume) is summarized in Figure 5.

Sediments from the Cretaceous/Tertiary boundary interval (Samples 113-690C-15X-4, 41 cm [247.81 mbsf] to -15X-4, 43 cm [247.83 mbsf]; see Pospichal and Wise, this volume, chapter 32) down to Sample 113-690C-18X-5, 36–38 cm (277.76 mbsf) are assigned to the *Nephrolithus frequens* Zone (Fig. 5).

The overlap of *Nephrolithus frequens* and *N. corystus* occurs in Samples 113-690C-18X-2, 127–129 cm (274.17 mbsf) to -18X-5, 36–38 cm (277.76). This interval, above the last occurrence of *Biscutum magnum*, defines the *N. corystus* Subzone. Assemblages of the interval above lack *N. corystus* and are thus assigned to the *Cribrosphaerella daniae* Subzone. The entire zone is characterized by assemblages similar to those of Site 689.

**Table 1. Distribution of calcareous nannofossils in ODP Hole 689B. Abundance: V = very abundant, A = abundant, C = common, F = few, R = rare, P = present. Preservation: G = good, M = moderate, P = poor. Reworked specimens are denoted by lower case letters.**

Age	Zone or Subzone	Core, section, interval (cm)	Depth (mbsf)	Abundance Preservation	<i>Acuturris scotus</i>	<i>Ahmuelerella octonadiata</i>	<i>Arkhangelskiella cymbiformis/specillata</i>	<i>A. cymbiformis</i>	<i>A. specillata</i>	<i>Aspidolithus parvus constrictus</i>	<i>Bidiscus rotatorius</i>	<i>Biscutum castrorum</i>	<i>B. constans</i>	<i>B. coronum</i>	<i>B. dissimilis</i>	<i>B. magnum</i>	<i>B. notaculum</i>	<i>Biscutum</i> sp.	<i>Broinsonia enormis</i>	<i>Centosphaera barbata</i>	
late Maestrichtian	<i>Nephrolithus frequens</i>	<i>Cribrosphaerella daniae</i>	25X-5, 89-90	233.50	A M	A F	A .	. .	. .	. .	. .	. .	. .	. .	. .	. .	. .	. .	. .	. .	
			25X-5, 129-130	233.90	A M	A F	A .	. .	. .	. .	. .	. .	. .	. .	. .	. .	. .	. .	. .	. .	. .
			25X-6, 61-62	234.72	A P	A .	A .	. .	. .	. .	. .	. .	. .	. .	. .	. .	. .	. .	. .	. .	. .
			26X-1, 30-32	236.61	A P	A .	A .	. .	. .	. .	. .	. .	. .	. .	. .	. .	. .	. .	. .	. .	. .
			27X-1, 33-35	246.34	A P	A P	A .	. .	. .	. .	. .	. .	R	P	. .	. .	. .	. .	. .	. .	. .
			27X-2, 32-34	247.83	V P	A .	A .	. .	. .	. .	. .	. .	F	. .	. .	. .	. .	. .	. .	. .	. .
			27X-3, 29-31	249.29	A P	A .	C .	. .	. .	. .	. .	. .	. .	. .	. .	. .	. .	. .	. .	P	. .
	<i>N. corystus</i>	27X, CC	255.60	A P	A P	C .	. .	. .	. .	. .	P	. .	. .	. .	. .	. .	. .	. .	. .	. .	
		28X-1, 29-31	255.90	A P	A R	C .	. .	. .	. .	. .	. .	. .	. .	. .	. .	P	. .	. .	. .	. .	
early Maestrichtian	<i>Biscutum magnum</i>	28X-1, 135-137	256.96	A P	A C	A .	. .	. .	p	. .	R	. .	. .	P	C	. .	. .	. .	. .		
		28X-2, 29-31	257.40	V M	A C	. .	A C	. .	. .	. .	. .	. .	. .	. .	P	C	P	F	. .	P	
		28X-3, 30-33	258.92	A M	A F	. .	C .	. .	. .	. .	. .	. .	F	. .	P	A	C	C	. .	P	
		28X-4, 28-30	260.39	A P	A F	C .	. .	. .	. .	. .	. .	F	. .	F	F	C	F	. .	. .	P	
		29X-1, 28-31	265.50	A P	C .	C .	. .	. .	. .	. .	. .	. .	. .	. .	P	C	F	C	. .	P	
		29X-2, 28-30	266.99	A M	C .	. .	C C	. .	. .	. .	. .	F	P	. .	F	A	P	C	. .	P	
	<i>Biscutum coronum</i>	29X-2, 130-132	268.01	A P	F F	C .	. .	. .	. .	. .	F	F	R	A	C	C	. .	. .	. .	P	
		29X-3, 28-30	268.49	A P	. .	F F	. .	. .	. .	P	. .	F	P	P	C	C	C	. .	. .		
		30X-1, 32-34	275.23	A P	A F	. .	C .	. .	. .	. .	C	P	P	F	F	F	. .	. .	. .		
		30X-2, 35-37	276.76	C P	C .	. .	R .	. .	. .	. .	. .	P	P	F	F	. .	. .	. .	. .		
		30X-3, 28-30	278.19	A P	A F	. .	F .	. .	. .	. .	F	P	P	F	R	. .	. .	. .	. .		
		30X-3, 110-112	279.01	A P	A .	F .	. .	. .	. .	. .	P	. .	F	. .	. .	. .	. .	. .	. .		
		30X, CC	284.50	C P	C R	F .	. .	. .	. .	. .	P	R	. .	F	. .	. .	. .	. .	. .		
		32X, CC	294.30	F P	F F	. .	. .	. .	. .	. .	. .	. .	. .	. .	. .	. .	. .	. .	P	. .	
		33X, CC	297.30	C P	C .	F .	. .	. .	. .	. .	. .	F	P	. .	F	P	. .	. .	F	. .	

Preservation of nannofossils in sediments of the *N. frequens* Zone is poor to moderate. Although most forms show secondary calcite overgrowth, recognition of individual species is not severely hindered. These overgrowths may be sufficient, however, to affect the stable isotope values on the fine carbonate fractions. Stott and Kennett (this volume, chapter 47) note a negative excursion followed by a return of positive  $\delta^{18}O$  values in the interval where preservation is poor. In addition a positive shift is noted above this, close to the K/T boundary. Serious consideration must be given to the problem of overgrowth affecting these stable isotope signals.

The interval from Section 113-690C-18X, CC (281.1 mbsf) to Sample 113-690C-20X-1, 133-135 cm (292.13 mbsf) corresponds to the *Biscutum magnum* Zone (Fig. 5). Preservation is improved through this interval and several more forms are identified here than at Site 689 (Table 1). *Biscutum magnum* is common to abundant along with *N. corystus*. *Acuturris scotus*, *Monomarginatus quaternarius*, *Lucianorhabdus cayeuxii*, *Psykto-sphaera firthii*, and *B. notaculum* are few to common. The LO of *B. magnum* corresponds to the FO of *N. frequens* in Sample 113-690C-18X-5, 36-38 cm.

Several reworked specimens of the Campanian species, *Aspidolithus parvus constrictus* were noted in Section 113-690C-18X, CC, suggesting that sediments older than Maestrichtian are present on Maud Rise. Instability of the Maestrichtian depositional regime on Maud Rise is indicated by folds and micro-faults within the sediments immediately above Core 113-690C-18X (Shipboard Scientific Party, 1988a, p. 192 and fig. 11). Un-

der these circumstances, downslope transport of sediment and reworking of nannofossils could be expected.

The *Biscutum coronum* Zone is comprised of sediments from the interval of Sample 113-690C-20X-2, 28-30 cm (292.58 mbsf) to -22X-5, 29-31 cm (316.39 mbsf) just above basalt (Fig. 5). In addition to the taxa listed above for this zone, the assemblage here includes rare to few *Octocylus magnus*, *Mono-marginatus pectinatus*, *Misceomarginatus pleniporus*, and *Z. diplogrammus*. Rare *Tranolithus phacelosus* are also noted in the lower part of this zone as at Site 689. *Psykto-sphaera firthii* first appears in the middle of this zone and is common to abundant. The upper range of *T. phacelosus* is used by Sissingh (1977) as a lower Maestrichtian marker. The interval is therefore assigned to the lower Maestrichtian part of the *B. coronum* Zone.

As at Site 689, holococcoliths are abundant and dominant near the base of the hole. Preservation is slightly better in Core 113-690C-22X, which facilitates better discrimination between *Acuturris* and *Lucianorhabdus*. Coccolith species diversity and overall abundance are much less at the base of this hole. Holococcoliths are discussed in more detail below.

## DISCUSSION

### Biostratigraphy

The lower part of the *Nephrolithus frequens* Zone proposed here can be roughly correlated with the *Arkhangelskiella cymbiformis* Zone (CC25) of Sissingh (1977), which is based on the gap interval from the LO of *Reinhardtites levis* to the FO of *N.*



Table 2. Distribution of calcareous nanofossils in ODP Hole 690C. Abundance: V = very abundant, A = abundant, C = common, F = few, R = rare, P = present. Preservation: G = good, M = moderate, P = poor. Reworked specimens are denoted by lower case letters.

Age	Zone or Subzone	Core, section, interval (cm)	Depth (mbsf)	Abundance	Preservation	<i>Acuturris scotus</i>	<i>Ahmuelerella octoradiata</i>	<i>Arkhangelskiella cymbiformis/specillata</i>	<i>A. cymbiformis</i>	<i>A. specillata</i>	<i>Aspidolithus parvus constrictus</i>	<i>Biantholithus sparsus</i>	<i>Bidiscus rotatorius</i>	<i>Biscutum boletum</i>	<i>B. castrorum</i>	<i>B. constans</i>	<i>B. coronum</i>	<i>B. dissimilis</i>	<i>B. magnum</i>	<i>B. notaculum</i>	<i>Biscutum</i> sp.	<i>Bronsonia enormis</i>	<i>Centosphaera barbata</i>	<i>Chiasiozygus garrisonii</i>	<i>Chiasiozygus</i> sp.	
late Maestrichtian	<i>Nephrolithus frequens</i>  <i>Cribrosphaerella daniae</i>	15X-4, 49-50	247.90	V M	A F A	.	.	.	.	.	P	.	.	C	.	.	.	.	.	p	.	.	.	C		
		15X-4, 53-54	247.99	V P	A F A	.	.	.	.	.	.	.	.	.	F	.	.	.	.	.	.	.	.	.	C	
		15X-4, 145-146	248.86	V M	A F A	.	.	.	.	.	.	.	.	.	R	.	.	.	.	.	.	.	.	.	F	
		15X-5, 27-28	249.18	V P	A F A	.	.	.	.	.	.	.	.	.	.	.	.	.	.	.	.	.	.	.	R	
		15X-5, 120-121	250.11	A P	A P A	.	.	.	.	.	.	.	.	.	.	.	.	.	.	.	.	.	.	.	P	
		16X, CC	261.80	V M	A F C	.	.	.	.	.	.	.	.	.	.	.	.	.	.	.	.	.	.	.	P	
		17X-1, 30-32	262.11	A M	A F A	.	.	.	.	.	.	.	.	.	F	.	.	.	.	.	.	.	.	.	P	
		17X-2, 30-32	263.61	V M	A . A	.	.	.	.	.	.	.	.	.	.	.	.	.	.	.	.	.	.	.	F	
		17X-3, 30-32	265.11	V M	A P A	.	.	.	.	.	.	.	.	.	P	P	.	.	.	.	.	.	.	.	P	
		17X, CC	271.40	A P	C P C	.	.	.	.	.	.	.	.	.	R	.	.	.	.	.	.	.	.	.	R	
				18X-2, 127-129	274.17	V P	A F A	.	.	.	.	.	.	.	P	.	.	.	.	.	F	.	.	.	.	.
				18X-3, 26-28	274.67	V P	A F A	.	.	.	.	.	.	P	.	R	.	.	.	.	F	.	.	.	.	.
				18X-4, 22-24	276.13	A P	C . C	.	.	.	.	.	.	.	R	.	.	.	.	.	F	.	.	.	.	.
				18X-5, 36-38	277.76	V P	C . C	.	.	.	.	.	.	.	P	.	.	.	.	.	P	F	.	.	.	.
		early Maestrichtian	<i>Biscutum magnum</i>	18X, CC	281.10	A M	C F . C F	f	.	.	.	.	.	.	.	.	P	P	F	F	F	.	.	.	.	.
				19X-1, 130-132	282.41	A M	C F . A	.	.	.	.	.	.	.	.	.	.	F	R	C	F	.	.	.	.	F
				19X-2, 130-132	283.91	V G	C C F . A P	.	.	.	.	.	.	P	.	.	.	R	.	R	A	F	.	.	.	F
				19X-3, 130-132	285.41	V G	C C C . C	.	.	.	.	.	.	.	.	.	.	R	.	F	A	F	.	.	.	C
19X-4, 127-130	286.90			V M	C C C . C F	.	.	.	.	.	.	.	.	.	.	R	.	F	A	F	.	.	P	C		
19X-5, 130-132	288.41			V M	C C C . A	.	.	.	.	.	.	.	.	P	.	F	.	F	A	A	.	.	.	F		
19X-6, 28-30	288.89			V M	C C C . A	.	.	.	.	.	.	.	R	.	.	F	.	F	A	C	.	.	.	C		
20X-1, 30-32	291.11			V G	C C C . A F	.	.	.	.	.	.	.	.	.	.	R	.	F	A	C	.	.	.	C		
20X-1, 133-135	292.14			V G	F C C . A F	.	.	.	.	.	.	.	.	.	.	P	P	A	A	P	.	.	.	C		
<i>Biscutum coronum</i>	20X-2, 28-30			292.59	V G	F C C . A C	r	.	.	.	.	.	.	.	.	F	F	F	A	A	C	.	.	.	C	
	20X-2, 124-126			293.55	V G	C C C . A C	.	.	.	.	.	.	.	.	.	.	F	C	C	A	A	C	.	.	.	C
	20X-3, 123-125			295.04	V G	C C C . C A	.	.	.	.	.	.	.	.	.	.	C	R	F	A	A	C	.	.	.	C
	20X-4, 104-106			296.35	V G	F A . C C C	r	.	.	.	.	.	.	.	.	.	F	F	F	A	A	A	.	.	.	C
	20X-5, 143-145			298.24	V G	F A . C C C	.	.	.	.	.	.	.	.	.	.	F	F	R	A	A	A	.	.	.	C
	20X, CC			300.40	V G	C A . C F	.	.	.	.	.	.	.	.	.	.	F	F	.	C	A	A	.	.	.	C
	21X-1, 131-133			301.72	V G	C A . A F	.	.	.	.	.	.	.	.	.	.	P	F	.	C	A	A	.	.	.	C
	21X-2, 29-31			302.20	V G	C C . A F	.	.	.	.	.	.	.	.	P	.	F	F	.	C	A	A	.	.	.	C
	21X-3, 28-30			303.69	V G	C A . A F	.	.	.	.	.	.	.	.	P	.	F	R	F	C	F	A	.	.	.	C
	21X-4, 8-10	304.99	V G	A A . A F	.	.	.	.	.	.	.	.	.	.	F	P	.	A	C	A	.	.	.	C		
	21X-5, 30-32	306.71	V M	A C . C F	.	.	.	.	.	.	.	.	.	.	C	.	P	C	C	.	.	.	.	C		
	21X, CC	310.10	A M	C C . C F	.	.	.	.	.	.	.	.	.	.	P	.	F	F	.	.	.	.	.	P		
	22X-1, 133-135	311.44	A M	A C . F F	.	.	.	.	.	.	.	.	.	.	C	.	F	C	P	.	.	.	.	P		
	22X-2, 133-135	312.94	A M	A C . F F	.	.	.	.	.	.	.	.	.	.	F	P	.	F	C	.	.	.	.	F		
	22X-3, 133-135	314.44	A M	A . . C F	p	.	.	.	.	.	.	.	.	.	C	.	F	C	.	.	R	.	R	.		
	22X-5, 29-31	316.40	A P	A . . C R	.	.	.	.	.	.	.	.	.	.	R	R	.	.	.	.	P	.	.	.		

was still able to piece together data from the Falkland Plateau and DSDP Sites in the Indian Ocean to derive a basis for a Campanian-Maestrichtian zonation (see discussion by Wise, 1988, which has been expanded here).

Also, the upper ranges of the austral forms, *Monomarginatus quaternarius*, *M. pectinatus*, and *Misceomarginatus pleniporus* could not be determined here. Wind and Wise (1983) had proposed that these species would be stratigraphically useful, especially in the interval encompassing the Campanian/Maestrichtian boundary. However, because of their inconsistent occurrence at Maud Rise, the usefulness of *M. pectinatus* and *M. pleniporus* could not be demonstrated.

It is hoped that with the additional recent drilling in the Southern Oceans (Leg 114 Scientific Party, 1987; plus ODP Legs 119-121), significant progress can be made toward refining the austral high latitude zonation scheme presented here. Higher

resolution for the Campanian-early Maestrichtian is much needed and should be provided by these later legs.

### Biogeography

The nanofossil assemblages of Sites 689 and 690 are quite similar to those described by Wise and Wind (1977) and Wise (1983) from the Falkland Plateau of the South Atlantic. Thus, the Falkland Plateau Biogeographic Province as defined by Wind (1979b) can be extended to the margins of East Antarctica. As shown in Table 3, except for a few cases, most of the taxa described in those studies were noted here. The absence of some of these forms may be the result of provinciality, latitudinal effects, or preservational factors.

As previously mentioned, the time-transgressive first occurrence of *Nephrolithus frequens*, as first suggested by Worsley and Martini (1970), and the absence of a gap between the FO of



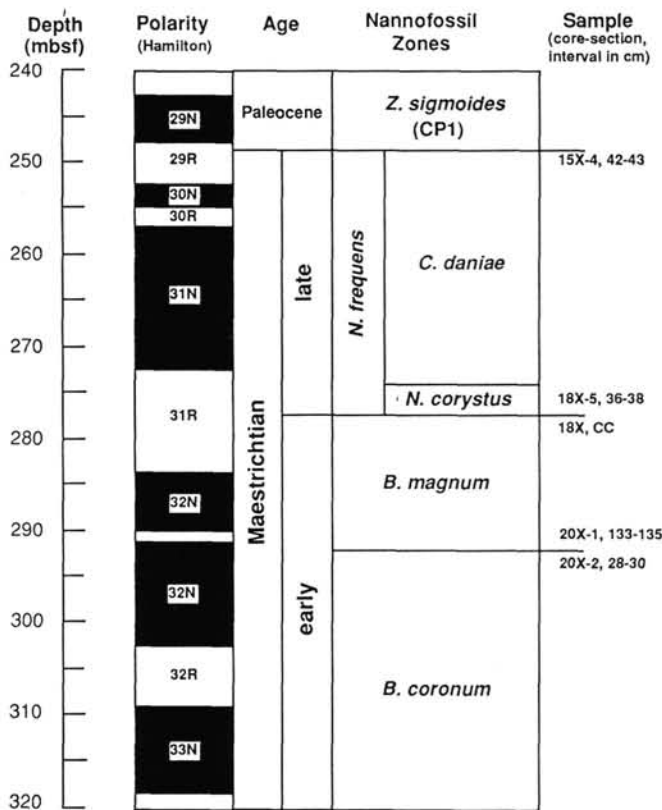


Figure 5. Summary of the calcareous nannofossil biostratigraphy of Hole 690C correlated with the magnetostratigraphy of Hamilton (this volume).

imately the same level as the FO of *N. frequens* in Chron 31N. At Site 605 (New Jersey continental margin, 38°N), Lang and Wise (1987) report LO of *R. anthophorus* in the uppermost Maestrichtian, well above the FO of *N. frequens* (Chron 30N), but reworking is suspected there as several other Campanian-lower Maestrichtian forms (e.g., *Eiffelithus eximius*) exhibit similar ranges. Although only a few sections are mentioned here, it is apparent that determination of the range and distribution of *Reinhardtites* is complicated by factors such as reworking and the limited availability of data.

The distribution of *Nephrolithus frequens*, which has a bipolar distribution and becomes increasingly rarer toward the Equator (Thierstein, 1981), is more easily documented in the Atlantic Ocean. Its FO at Sites 689 and 690 on Maud Rise (65°S), in about the middle of Chron 31R, corresponds to the LO of *Reinhardtites levis* and *Biscutum magnum*. The LO of *N. corystus* occurs near the top of Chron 31R at both sites. On the Walvis Ridge, the FO of *N. frequens* is reported in Chron 31N at Site 524 (Poore et al., 1984) and in Chron 30N, at Site 525 (Chave, 1984). At Site 516 (Rio Grande Rise, 30°S), Hamilton and Suzumov (1983) correlate the base of the *N. frequens* Zone to combined Chrons 30 and 31. *Nephrolithus corystus* was not reported from the Walvis Ridge sites and *N. frequens* was not observed at low latitude Site 530 (Stradner and Steinmetz, 1984). At North Atlantic Sites 384 and 387, the FO of *N. frequens* is in Chron 31N (Okada and Thierstein, 1979). It should be noted that many workers might have included *N. corystus* within *N. frequens* as Worsley (1974) more than likely did when he reported *N. frequens* "et al." from lower Maestrichtian polar shelf sections (see discussion in Huber et al., 1983).

From the few sites documented here, the time-transgressive occurrence of *N. frequens* can be demonstrated, at least for the

Table 3. Comparison of occurrence and abundance of Campanian-Maestrichtian calcareous nannofossil taxa from Maud Rise with those in Falkland Plateau assemblages. A = abundant, C = common, F = few, (\*) = not reported or observed.

Falkland Plateau Province Flora	Average relative abundance	
	Sites 327, 511	Sites 689, 690
<i>Acuturrus scotus</i>	C-A	A
<i>Ahmullerella octoradiata</i>	A	C-A
<i>Arhangelskiella cymbiformis/specillata</i>	C	C-A
<i>Bidiscus rotatorius</i>	R-F	R
<i>Biscutum boletum</i>	R	R
<i>B. coronum</i>	C	F-C
<i>B. dissimilis</i>	R-C	R-F
<i>B. magnum</i>	C	C
<i>B. notaculum</i>	C-A	R-C
<i>Boletuvelum candens</i>	R-F	*
<i>Broinsonia enormis</i>	R-C	R
<i>B. verecundia</i>	R-C	*
<i>Centosphaera barbata</i>	F	R
<i>Chiasozygus garrisonii</i>	C	C
<i>Corollithion rhombicum</i>	R	R
<i>Cretarhabdus conicus</i>	C	C
<i>C. surirellus</i>	R	R-F
<i>Cribrosphaerella daniae</i>	*	C
<i>C. ehrenbergii</i>	A	C
<i>Cruciplacolithus</i> sp. cf. <i>C. inaequus</i>	*	R
<i>Cyclagelosphaera margarellii</i>	R	R
<i>Eiffelithus turriseiffelii</i>	A	C
<i>Gartnerago</i> spp.	C-A	C
<i>Kampfnerius magnificus</i>	A	A
<i>Lapideacassis mariae</i>	R-F	R-F
<i>L. tricornis</i>	R	R-F
<i>Lucianorhabdus arborius</i>	R-C	R
<i>L. arcuatus</i>	F-C	R
<i>L. cayeuxii</i>	C	F-C
<i>Micula decussata</i>	F-C	F
<i>Misceomarginatus pleniporus</i>	C	R
<i>Monomarginatus pectinatus</i>	C	R
<i>M. quaternarius</i>	C	F-C
<i>Neocrepidolithus watkinsii</i>	*	C
<i>Nephrolithus corystus</i>	A	A
<i>N. frequens</i>	A	A
<i>Octocyclus magnus</i> (= <i>O. reinhardtii</i> )	R-C	R
<i>Okkolithus australis</i>	R	*
<i>Orastrum asarotum</i>	R-F	*
<i>Phanulithus additus</i>	R	*
<i>P. obscurus</i>	C	F-C
<i>P. ovalis</i>	R	*
<i>Pharus simulacrum</i>	R-F	*
<i>Prediscosphaera cretacea</i>	C-A	C-A
<i>P. spinosa</i>	C-A	C-A
<i>P. stoveri</i>	C-A	A
<i>Reinhardtites</i> sp. aff. <i>R. anthophorus</i>	R	R
<i>R. levis</i>	C	C
<i>Russellia multiplus</i>	F-C	*
<i>Teichorhabdus ethmos</i>	R	F
<i>Thoracosphaera</i> sp.	F	R
<i>Tranolithus phacelosus</i> (= <i>T. orionatus</i> )	F-C	R
<i>Vekshinella</i> spp.	F-C	F-C
<i>Watznaueria barnesae</i>	F-C	F
<i>Zygodiscus compactus</i> (= <i>Z. bicrescenticus</i> )	F-C	F-C
<i>Z. diplogrammus</i>	C	F
<i>Z. sigmoides</i>	F-C	C
<i>Z. spiralis</i>	R-C	F-C

South Atlantic (Fig. 6). However, more paleomagnetic and stratigraphic data is necessary to support this scenario on a global basis. Additional stratigraphic data on *Reinhardtites levis* is also necessary to support assumptions concerning the LO of this species as conveyed in this report. Figure 7 summarizes our idealized concept of the relationships between *N. frequens*, *N. corystus*, and the key species of the late Maestrichtian.

The northward migration of *Nephrolithus frequens* may indicate a global cooling in the late Maestrichtian (Worsley, 1974)

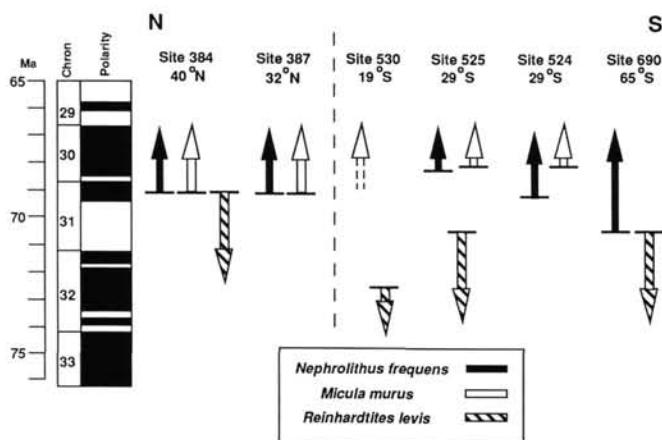


Figure 6. First occurrence of *Nephrolithus frequens* (black) and *Micula murus* (white) and the last occurrence of *Reinhardtites levis* (striped) from various Atlantic Ocean DSDP and ODP sites correlated with the magnetic time scale of Kent and Gradstein (1985). See text for references of each site.

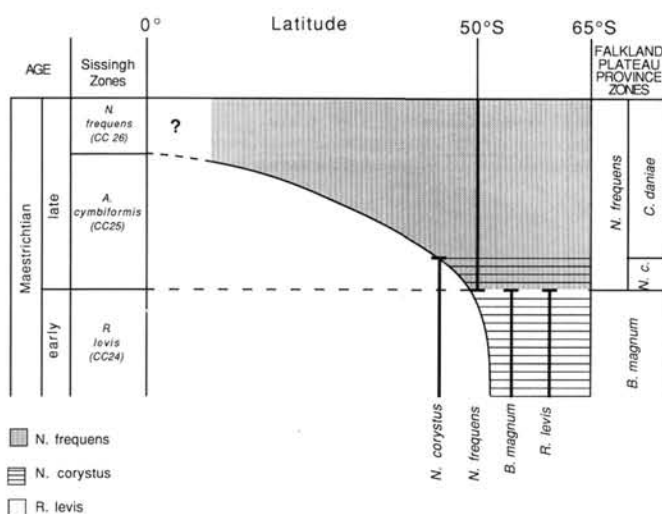


Figure 7. Proposed relationship between *Nephrolithus frequens*, *N. corystus*, and selected taxa correlated to latitude and age.

with *N. frequens* simply following the cooler water masses as they expanded toward the equator. The eventual geographic extent of *N. frequens* remains uncertain, especially in regards to its occurrence at the Equator and in the Northern Hemisphere. *Nephrolithus corystus* has only been reported from austral sections, and if *N. frequens* developed from this form and migrated northward across the Equator and into the northern latitudes, its first occurrence there would be later. For example, at Site 384 (40°N), the FO of *N. frequens* is in Chron 31N as opposed to Chron 31R on Maud Rise. Thus, a gap between the LO of *Reinhardtites levis* and *N. frequens* would be expected in all northern latitude sections, provided that the LO of the former is considered globally synchronous, which is not supported by data presented in Figure 6. The LO of *Reinhardtites* ranges from Chron 32N at Site 530 of the South Atlantic to Chron 31N at North Atlantic Sites 384 and 387.

An alternate hypothesis for the relationship between *N. frequens* and *R. levis* is that a hiatus exists at those sites where there is no gap between their first and last occurrences. How-

ever, a hiatus during this interval is difficult to reconcile since it is apparently not supported by foraminiferal or paleomagnetic data from these sections.

### Oldest Nannofossils on Maud Rise

The oldest nannofossils recovered on Maud Rise are the Campanian species, *Aspidolithus parvus constrictus*. A few specimens of this Campanian index taxon were present as reworked forms near the top of the *Biscutum magnum* Zone, several cores above the bottom of both Holes 689B and 690C; only very rare occurrences were recorded in two samples from the underlying *B. coronum* Zone of Site 690. These sporadic occurrences, combined with the observation that only very rare specimens of the lower Maestrichtian marker species, *Tranolithus phacelosus* are present near the bottom of Holes 689B and 690C, suggest that although Campanian sediments may be present elsewhere on Maud Rise, they were not cored during Leg 113. Furthermore, from recent detailed work on Campanian-Maestrichtian nannofossils from Algeria, Ghlis et al. (1988) suggest that *Eiffelithus eximius* and *Broinsonia parca* (= *A. parvus*) range into the lower Maestrichtian. Therefore, even if these datums were reached in these two holes, this would not necessarily mean that the Campanian was penetrated. However, Huber (this volume) suggests a Campanian age for the bottom of Hole 689B based on an extrapolation of planktonic foraminiferal datums on an age/depth plot. He, as do we, note that the bottoms of both holes are close to the Campanian/Maestrichtian boundary.

As previously mentioned, we attribute the presence of the Campanian nannofossil species we observed to downslope transport. More specimens were noted at Site 690, which lies on the southwest flank of Maud Rise, downslope from Site 689 (Fig. 2). An age of Campanian for the oldest sediments of the rise would be more consistent with the predicted age of the basement. The Leg 113 Shipboard Scientific Party (1988a, p. 184) reports that the presumed basement age for Maud Rise is middle Cretaceous (Cenomanian?), and that it would have been subaerial for about 10 m.y. after its formation.

### Holococcoliths and Paleodepths

Several holococcolith species are noted in the Maestrichtian sediments of Maud Rise. These include *Acuturris scotus* (the most abundant form through the entire interval), *Lucianorhabdus cayeuxii*, *L. arcuatus*, and *Phanulithus obscurus*. In poorly preserved material it was difficult to distinguish *A. scotus* (Pl. 9, Figs. 6a, b) from species of *Lucianorhabdus* (Pl. 9, Figs. 7, 9, 10) under the light microscope. *Acuturris scotus*, which normally has a needle shape, can resemble its counterpart when the narrow pointed end is broken off (see Pl. 9, Fig. 11a, b). Both forms are also subject to excessive overgrowth, further complicating their identification. Thus, estimations of the species abundances may not be as precise where preservation is poor. A review of Mesozoic holococcoliths is given by Wind and Wise (1978).

In the lower portion of the section, where coccoliths are much less common, the holococcoliths (mostly *A. scotus*) remain abundant and attain rock forming proportions (Pl. 9, Fig. 11a). This is best displayed in Core 113-690C-22X and Cores 113-689B-30X through -33X.

Holococcoliths are generally considered marginal or near-shore forms associated with shallow water deposits. Maud Rise is a fairly shallow aseismic platform in the Weddell Sea (Fig. 2), quite remote from the continent. The present depth of the rise near the crest at Site 689 is 2080 m; downslope at Site 690, the depth is 2914 m. The ridge is estimated to have been formed sometime during the middle to Late Cretaceous, no later than Campanian time. It would have been at shallower depths during its early history. Benthic foraminiferal data suggest paleodepths

of ~500–1000 m for the oldest sediments recovered at Site 689 and ~1500 m for Site 690 (see Thomas, this volume). The presence of abundant shallow water holococcoliths in sediments of Maestrichtian through middle Eocene age supports a model calling for the slow subsidence of an initially very shallow volcanic platform.

**SYSTEMATIC PALEONTOLOGY**

Species found in this study are listed in the Appendix. The range charts of Tables 1 and 2 provide abundance, preservation, and stratigraphic information for all individual taxa. The taxa below are listed alphabetically by generic epithets.

Genus *NEOCREPIDOLITHUS* Romein (1979)  
*Neocrepidolithus watkinsii* Pospical and Wise, n. sp.  
 (Pl. 7, Fig. 1)

**Diagnosis.** A large species of *Neocrepidolithus* with an eiffellithid rim constructed of thin rectangular laths imbricated in a clockwise direction. The proximal side is constructed of a thin cycle of elements which form the basal plate. In distal view, the solid central area is composed of blocky elements that form a ridge along the major and minor axis but leave a depression in the center.

**Description.** An elliptical coccolith with a relatively thick outer rim constructed of ~50–55 strongly imbricated rectangular laths. The solid central area of the distal side consists of a number of thin overlapping elements. The elements form a ridge along the major and minor axes within the central area. Under cross-polarized light, the rim is birefringent, as is the cross formed by elements of the central area. In plain light, the outline of this cross can also be discerned, and it is quite distinctive in phase contrast light.

**Remarks.** The species is named for Dr. David K. Watkins in honor of his many valuable contributions to this subdiscipline of micropaleontology. In general, most other species of this genus are smaller than *N. watkinsii*, but are found in uppermost Maestrichtian and lower Tertiary sediments. The type species for the genus, *Neocrepidolithus neocrassus* (Perch-Nielsen, 1968; Romein, 1979), is a 4–7 μm form found in Danian sediments. In addition, the height of the rim of the species described here is proportionately less than for other species of the genus.

Specimens of *N. watkinsii* are differentiated from species of *Vagapilla* Bukry (1969) in having the central area completely filled with crystalline elements, whereas the central areas of species such as *Vagapilla aachena* (Bukry) have open quadrants separated by cross bars. *Neocrepidolithus watkinsii* is, on average, several microns larger than species of *Vagapilla*.

**Occurrence.** Few to common in the Maestrichtian *Biscutum coronum* and *B. magnum* Zones of Maud Rise. Also present through the same interval in sediments of Broken Ridge and elsewhere in the Indian Ocean.

**Size.** Length 9–13 μm (Holotype, 10.0 μm, width, 6.3 μm).

**Holotype.** Plate 7, Figures 1a–b.

**Isotype.** Plate 7, Figures 1c–e.

**Type locality.** ODP Sample 113-690C-21X-3, 29–30 cm.

Genus *NEPHROLITHUS* Görka, 1957  
*Nephrolithus frequens frequens* Görka

- Nephrolithus frequens* Görka, 1957, p. 263, pl. 5, fig. 7.
- Nephrolithus barbarae* Görka, 1957, p. 264, pl. 5, fig. 9.
- Nephrolithus furcatus* Görka, 1957, p. 263, pl. 5, fig. 8.
- Nephrolithus trientis* Görka, 1957, p. 263, pl. 5, fig. 10.
- Nephrolithus gorkae* Aberg, 1966, p. 65–67, pl. 1; pl. 2, figs. 1–5; pl. 3, figs. 1–5; text-fig. 1.

*Nephrolithus frequens* (Reinhardt and Görka, 1967)  
*miniporus* Pospical and Wise emend., n. comb.  
 (Figs. 8A–C, E)

*Nephrolithus miniporus* Reinhardt and Görka, 1967, p. 246–247, pl. 32, fig. 11, pl. 33, fig. 5.

**Diagnosis.** Reniform to elliptical subspecies of *Nephrolithus frequens frequens* having only two holes within the central area.

**Description.** The description follows that of Wind (1983) for *N. f. frequens*. This new subspecies retains the same rim structure as *N. f. frequens*, but is generally smaller in size. The outer rim is constructed of inclined rectangular elements. The distinguishing feature of this form is in the central area, which is characterized by only two holes ringed by 7–

8 calcite rhombs. The holes of the central area are distinct in phase contrast and cross polarized light (Figs. 8B, C). The shape of *N. f. miniporus* is either the characteristic “kidney bean” shape or more elliptical. The size ranges from 4 to 7 μm.

**Remarks.** Reinhardt and Görka (1967) originally defined the species, *N. miniporus*, as having 2–4 holes in the central area. We restrict *N. f. miniporus* to forms with only two holes because we observed no specimens with three holes and include those with four or more within *N. f. frequens*. However, when observed under the light microscope, some specimens of *N. f. miniporus* (with two holes) appear to have a third smaller perforation located between the two major holes but slightly offset. This is considered to be an optical illusion since none of these three-holed forms could be found using the scanning electron microscope.

Figure 9 shows a comparison of the abundances of the species of *Nephrolithus*, *N. f. frequens*, *N. f. miniporus*, and *N. corystus*. The percentages are based on a smear slide count of 100 specimens of *Nephrolithus* from Hole 690C. The smaller forms (4–5 μm) of *N. f. miniporus* are more common in the *N. corystus* Subzone. Specimens are generally larger in uppermost Maestrichtian sediments and the form is dominant over *N. f. frequens* for a short interval from 265.11 mbsf to 261.80 mbsf.

In the light microscope, early small forms are difficult to distinguish from small *N. corystus*, especially when preservation is poor. In order to differentiate these small forms, it is generally necessary to observe the central areas using scanning electron microscopy. For example, Figure 8D is a small form, probably *N. corystus*. Although the pores have been closed by overgrowth, the smaller crystals comprising the central area and the vestiges of a central spine are more characteristic of this species. Figure 8E, similarly a very small species considered to belong to *N. f. miniporus*, is characterized by blunt crystals in the central area and no apparent spine.

In regard to the evolution of *Nephrolithus frequens frequens*, the small forms of *N. f. miniporus* (Fig. 8E) may have evolved from the smaller forms of *N. corystus* (Fig. 8D), thereby providing the link between these two taxa. Unfortunately, at present, this can only be speculation because of poor preservation in the samples encompassing this critical transition.

**Occurrence.** Common to abundant in the upper Maestrichtian of Maud Rise, Weddell Sea.

**Size.** 4–7 μm.

Genus *PSYKTOSPHAERA* Pospical and Wise, n. gen.  
 (Pl. 4, Figs. 1a–d)

**Type species.** *Psyktosphaera firthii* Pospical and Wise, n. sp.

**Diagnosis.** Elliptical coccoliths in which the distal shield is veneered by an outer rim of ~40 or more strongly imbricate thin laths that surround an outer central area consisting of long thin vertical lath-shaped elements arranged in a concentric pattern around a perforate inner central area.

**Description.** See description of type species.

**Remarks.** The name is from the Greek meaning “cool sphere.”

**Differentiation.** In the light microscope, the outer rim of *Psyktosphaera* resembles that of *Cribrrosphaerella*, particularly *Cribrrosphaerella daniae* Perch-Nielsen (1973) (compare Pl. 4, Figs. 1d and 2c). However, a set of thin, strongly imbricate lath-shaped elements veneer the outer rim of *Psyktosphaera* (compare Pl. 4, Figs. 1a and 2a). The central area *C. daniae* (pl. 1, fig. 1; Perch-Nielsen, 1973) consists of numerous granular crystals and has no discernable pattern of perforations, which differs from the central area of *Psyktosphaera* as described for the type species below.

*Psyktosphaera firthii* Pospical and Wise, n. sp.  
 (Pl. 5, Figs. 1a–d)

*Cribrrosphaerella daniae*, Wind (1979a), p. 250, pl. 4, figs. 1–3.

**Diagnosis.** Medium sized, elliptical species of *Psyktosphaera* with a distal shield consisting of a perforate inner central area, an outer central area of concentrically arranged, vertical elongate elements, and an outer rim of strongly imbricate lath-shaped elements that veneer a set of thicker, subvertical elements.

**Description.** The distal shield is comprised of an outer rim of two cycles and a perforate inner central area surrounded by concentrically arranged elongate elements. The outer rim of the distal shield is composed of thin veneer of ~40 or more lath-shaped elements strongly im-

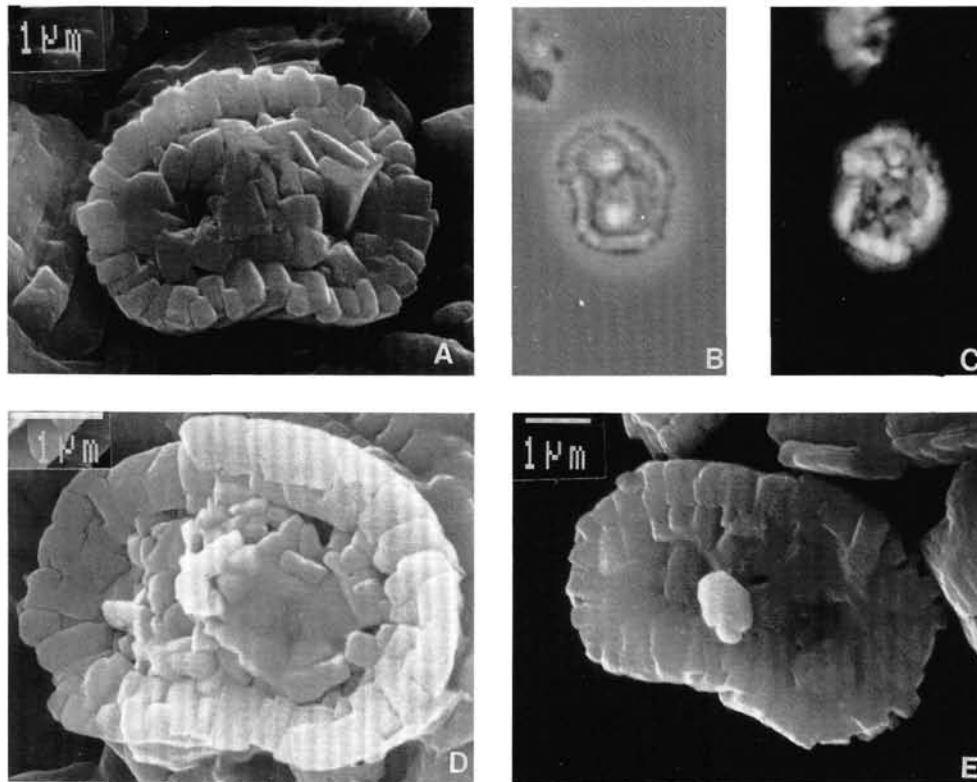


Figure 8. **A.** Scanning electron micrograph (SEM) of *Nephrolithus frequens miniporus* emend., n. comb., Sample 113-690C-18X-3, 26–28 cm. **B, C.** Phase contrast and cross polarized light micrographs, respectively of *N. f. miniporus* emend. ( $\times 2250$ ), Sample 113-690C-15X-4, 151–152 cm. **D.** SEM of *N. corystus*, Section 113-690C-18X, CC. **E.** SEM of *N. f. miniporus* emend., Sample 113-690C-17X-3, 30–32 cm. Note 1  $\mu\text{m}$  scale bar on scanning electron micrographs.

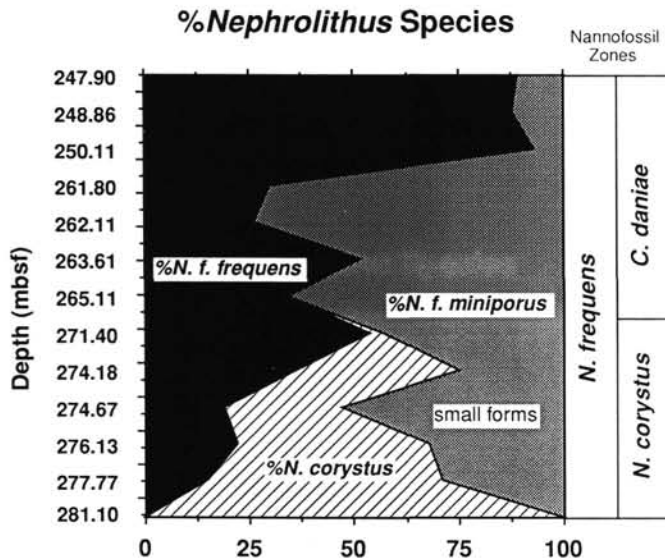


Figure 9. Percent abundance of individual species of the genus *Nephrolithus* in Sample 113-690C-15X-4, 49–50 cm (247.90 mbsf) down to Section 113-690C-18X, CC (281.10 mbsf). Samples are designated on graph in meters below sea floor (mbsf). Refer to Table 2 for ODP sample designations.

bricated in the sinistral direction and underlain by an additional cycle of equal diameter. The latter is composed of blocky rather than lath-shaped elements that exhibit only a slight sinistral imbrication. The proximal shield is composed of a single cycle of elements similar to the blocky elements of the outer distal shield. The diameter of the cycle of elements comprising the proximal shield is slightly less than that of the distal shield.

The outer central area of the distal shield is composed of thin, elongate vertical elements, which vary in length and are arranged in a concentric pattern around the inner central area. The inner central area is characterized by numerous perforations. The number of perforations ranges from ~8 to 25 depending on the size of the specimen. In distal view each perforation is ringed by four thin triangular elements which taper and slant toward the perforation.

In phase contrast light, the rim of *P. firthii* is dark (Pl. 4, Fig. 1d), and in cross polarized light, the rim displays a low order (gray) of birefringence. In cross polarized light, the outer cycle of elements within the central area display a similar order of birefringence, and the perforate inner central area appears granular (Pl. 4, Fig. 1c).

**Remarks.** The species is named after dual nannofossil-palynomorph micropaleontologist, Dr. John V. Firth, for his contributions to Maestrichtian biostratigraphy. Transmission electron micrographs from Wind (1979a, unpubl. dissert.) were used for the description of the proximal shield. As mentioned above, *Psykto-sphaera firthii* resembles *Cribrosphaerella daniae* Perch-Nielsen (1973) in the light microscope. The rim structure of these two forms is similar except for the presence of the thin veneer of strongly imbricate elements on the distal side of *P. firthii*. The central area of each form is clearly different as described above. Where preservation is poor, these two forms may be difficult to distinguish in the light microscope. However, despite poor preservation, they are fairly distinct in the SEM.

**Occurrence.** *Psykto-sphaera firthii* first appears in the middle of the lower Maestrichtian portion of the *Biscutum coronum* Zone in Hole

690C (Table 2) of Maud Rise. Specimens are common to abundant in this zone and in the overlying *B. magnum* Zone. An overlap in range between this species and *C. daniae* occurs in the upper part of the *B. magnum* Zone. In the section at Site 689, where preservation is poor, few *P. firthii* were noted in only one sample from the *B. coronum* Zone (Table 1). Wind (1979a), who illustrated this form as *C. daniae*, reported a similar stratigraphic distribution from Site 327 on the Falkland Plateau.

**Size.** 9–10  $\mu\text{m}$  (Holotype, 9.7  $\mu\text{m}$ ).

**Holotype.** Plate 4, Figure 1a.

**Isotype.** Plate 4, Figures 1b–d.

**Type locality.** ODP Sample 113-690C-19X-2, 130–132 cm.

### ACKNOWLEDGMENTS

This paper was excerpted from a thesis (Pospical, 1989) submitted in partial fulfillment of the Master of Science degree at Florida State University. Mr. Walter W. Thorner III assisted with constructing Figure 7. We thank our Leg 113 collaborators for helpful discussions. We also thank Drs. Hans Thierstein and Thomas R. Worsley whose comments and suggestions helped improve this manuscript. The study was supported by National Science Foundation grant DPP-8414268, Leg 113 USSAC Funds, an equipment grant from the Amoco Foundation, and a partial Aylesworth Foundation fellowship to J.P.P.

### REFERENCES

- Barker, P. F., Dalziel, I.W.D., et al., 1977. *Init. Repts. DSDP*, 36: Washington (U.S. Govt. Printing Office).
- Barker, P. F., Kennett, J. P., et al., 1988. *Proc. ODP, Init. Repts.*, 113: College Station, TX (Ocean Drilling Program).
- Cepek, P. and Hay, W. W., 1969. Calcareous nannoplankton and biostratigraphic subdivision of the Upper Cretaceous. *Trans. Gulf Coast Assoc. Geol. Soc.*, 19:323–336.
- Chave, A. D., 1984. Lower Paleocene-Upper Cretaceous magnetostratigraphy, Sites 525, 527, 528, and 529, Deep Sea Drilling Project Leg 74. In Moore, T. C., Jr., Rabinowitz, P. D., et al., *Init. Repts. DSDP*, Leg 74: Washington (U.S. Govt. Printing Office), 525–531.
- Hamilton, N., and Suzyumov, A. E., 1983. Late Cretaceous magnetostratigraphy of Site 516, Rio Grande Rise, southwestern Atlantic Ocean, Deep Sea Drilling Project, Leg 72. In Barker, P. F., Carlson, R. L., Johnson, D. A., et al., *Init. Repts. DSDP*, 72: Washington (U.S. Govt. Printing Office), 723–730.
- Hay, W. W., 1970. Calcareous nannofossils from cores recovered on Leg 4. In Bader, R. G., Gerard, R. D., et al., *Init. Repts. DSDP*, 4: Washington (U.S. Govt. Printing Office), 455–501.
- Huber, B. T., Harwood, D. M., and Webb, P. N., 1983. Upper Cretaceous biostratigraphy of Seymour Island, Antarctic Peninsula. *U.S. Antarctic J. Rev.*, 72–74.
- Kent, D. V., and Gradstein, F. M., 1985. A Cretaceous and Jurassic geochronology. *Geol. Soc. Am. Bull.*, 96:1419–1427.
- Lang, T. H., and Wise, S. W., 1987. Neogene and Paleocene-Maestrichtian calcareous nannofossil stratigraphy, Deep Sea Drilling Project Sites 604 and 605, upper continental rise off New Jersey: sedimentation rates, hiatuses, and correlations with seismic stratigraphy. In van Hinte, J. E., Wise, S. W., Jr. et al., *Init. Repts. DSDP*, 93: Washington (U.S. Govt. Printing Office), 661–681.
- Loeblich, A. R., Jr., and Tappan, H., 1966. Annotated index and bibliography of the calcareous nannoplankton, I. *Phycologia*, 5:81–216.
- \_\_\_\_\_, 1968. Annotated index and bibliography of the calcareous nannoplankton, II. *J. Paleontol.*, 42:584–598.
- \_\_\_\_\_, 1969. Annotated index and bibliography of the calcareous nannoplankton, III. *J. Paleontol.*, 43:568–588.
- \_\_\_\_\_, 1970a. Annotated index and bibliography of the calcareous nannoplankton, IV. *J. Paleontol.*, 44:558–574.
- \_\_\_\_\_, 1970b. Annotated index and bibliography of the calcareous nannoplankton, V. *Phycologia* 9:157–174.
- \_\_\_\_\_, 1971. Annotated index and bibliography of the calcareous nannoplankton, VI. *Phycologia*, 10:315–339.
- \_\_\_\_\_, 1973. Annotated index and bibliography of the calcareous nannoplankton, VII. *J. Paleontol.*, 47:715–759.
- Ludwig, W. J., Krashennnikov, V. A., et al., 1983. *Init. Repts. DSDP*, 71: Washington (U.S. Govt. Printing Office).
- Manivit, H., 1984. Paleogene and Upper Cretaceous calcareous nannofossils from Deep Sea Drilling Project Leg 74. In Moore, T. C., Jr., Rabinowitz, P. D., et al., *Init. Repts. DSDP*, Leg 74: Washington (U.S. Govt. Printing Office), 475–499.
- Okada, H., and Thierstein, H. R., 1979. Calcareous nannoplankton-Leg 43, Deep Sea Drilling Project. In Tucholke, B. E., Vogt, P. R., et al., *Init. Repts. DSDP*, 43: Washington (U.S. Govt. Printing Office), 507–573.
- Perch-Nielsen, K., 1968. Der Feinbau und die Klassifikation der Coccolithen aus dem Maastrichtien von Dänemark. *Ket Kongel. Danske Vidensk. Selskab Biolog. Skrift.*, 16:1–96.
- \_\_\_\_\_, 1973. Neue coccolithen aus dem Maastrichtien von Dänemark, Madagaskar und Ägypten. *Bull. Geol. Soc. Denmark*, 22: 306–333.
- \_\_\_\_\_, 1979a. Calcareous nannofossil zonation at the Cretaceous/Tertiary boundary in Denmark. In Birkelund, T., and Bromley, R. G. (Eds.), *Cretaceous-Tertiary Boundary Events*, Vol. 1: Copenhagen (Univ. of Copenhagen), 115–135.
- \_\_\_\_\_, 1979b. Calcareous nannofossils at the Cretaceous/Tertiary boundary near Biarritz, France. In Christensen, W. K., and Birkelund, T. (Eds.), *Cretaceous-Tertiary Boundary Events*, Vol. II: Copenhagen (Univ. of Copenhagen), 151–155.
- \_\_\_\_\_, 1979c. Calcareous nannofossils in Cretaceous/Tertiary boundary sections in Denmark. In Christensen, W. K., and Birkelund, T. (Eds.), *Cretaceous-Tertiary Boundary Events*, Vol. II: Copenhagen (Univ. of Copenhagen), 120–126.
- \_\_\_\_\_, 1985. Mesozoic calcareous nannofossils. In Bolli, H. M., Saunders, J. B., and Perch-Nielsen, K. (Eds.), *Plankton Stratigraphy*: Cambridge (Cambridge Univ. Press), 329–426.
- Percival, S. F., Jr., 1984. Late Cretaceous to Pleistocene calcareous nannofossils from the South Atlantic, Deep Sea Drilling Project Leg 73. In Hsü, K. H., LaBrecque, J. L., et al., *Init. Repts. DSDP*, 73: Washington (U.S. Govt. Printing Office), 391–424.
- Poore, R. Z., Tauxe, L., Percival, S. F., LaBrecque, J. L., Wright, R., Petersen, N. P., Smith, C. C., Tucker, P., and Hsü, K. J., 1984. Late Cretaceous-Cenozoic magnetostratigraphic and biostratigraphic correlations for the South Atlantic Ocean, Deep Sea Drilling Project Leg 73. In Hsü, K. H., LaBrecque, J. L., et al., *Init. Repts. DSDP*, 73: Washington (U.S. Govt. Printing Office), 645–655.
- Pospical, J. J., 1989. Maestrichtian to middle Eocene calcareous nannofossils, Maud Rise, Weddell Sea, Antarctica [M.S. thesis]. Florida State Univ., Tallahassee.
- Reinhardt, P., and Görka, H., 1967. Revision of some Upper Cretaceous coccoliths from Poland and Germany. *Neues Jahrb. für Geol. und Paleontol.*, Abh., 124:240–256.
- Romein, A.J.T., 1979. Lineages in early Paleogene calcareous nannoplankton. *Utrecht Micropaleontol. Bull.*, 22:1–231.
- Roth, P. H., 1978. Cretaceous nannoplankton biostratigraphy and oceanography of the Northwestern Atlantic Ocean. In Benson, W. E., Sheridan, R. E., et al., *Init. Repts. DSDP*, 44: Washington (U.S. Govt. Printing Office), 731–759.
- Roth, P. H., and Bowdler, J. L., 1981. Middle Cretaceous calcareous nannoplankton biogeography and oceanography of the Atlantic Ocean. In Warme, J. E., Douglas, R. G., and Winterer, E. L. (Eds.), *The Deep Sea Drilling Project: A Decade of Progress*. Soc. Econ. Paleontol. Mineral, Spec. Publ., 32:517–546.
- Shipboard Scientific Party, 1988a. Site 690. In Barker, P. F., Kennett, J. P., et al., *Proc. ODP, Init. Repts.*, 113: College Station, TX (Ocean Drilling Program), 183–292.
- \_\_\_\_\_, 1988b. Site 698. In Ciesielski, P. F., Kristoffersen, Y., et al., 1988b. *Proc. ODP, Init. Repts.*, 114: College Station, TX (Ocean Drilling Program), 87–150.
- Sissingh, W., 1977. Biostratigraphy of Cretaceous calcareous nannoplankton. *Geol. Mijnbouw*, 56:37–65.
- Steinmetz, J. C., 1984a. Bibliography and taxa of calcareous nannoplankton-III. *Int. Nannoplankton Assoc. Newsl.*, 6:6–37.
- \_\_\_\_\_, 1984b. Bibliography and taxa of calcareous nannoplankton-IV. *Int. Nannoplankton Assoc. Newsl.*, 6:55–81.
- \_\_\_\_\_, 1985a. Bibliography and taxa of calcareous nannoplankton-V. *Int. Nannoplankton Assoc. Newsl.*, 7:5–28.
- \_\_\_\_\_, 1985b. Bibliography and taxa of calcareous nannoplankton-IV. *Int. Nannoplankton Assoc. Newsl.*, 7:122–144.
- \_\_\_\_\_, 1986. Bibliography and taxa of calcareous nannoplankton-VII. *Int. Nannoplankton Assoc. Newsl.*, 8:66–82.
- \_\_\_\_\_, 1987a. Bibliography and taxa of calcareous nannoplankton-IX. *Int. Nannoplankton Assoc. Newsl.*, 9:8–26.

- \_\_\_\_\_, 1987b. Bibliography and taxa of calcareous nannoplankton. *X. Int. Nannoplankton Assoc. Newsl.*, 9:79-105.
- \_\_\_\_\_, 1988a. Bibliography and taxa of calcareous nannoplankton. *XI. Int. Nannoplankton Assoc. Newsl.*, 10:7-28.
- \_\_\_\_\_, 1988b. Bibliography and taxa of calcareous nannoplankton. *XII. Int. Nannoplankton Assoc. Newsl.*, 10:60-80.
- \_\_\_\_\_, 1989. Bibliography and taxa of calcareous nannoplankton. *XII. Int. Nannoplankton Assoc. Newsl.*, 11:6-20.
- Stradner, H., and Steinmetz, J., 1984. Cretaceous calcareous nannofossils from the Angola Basin, Deep Sea Drilling Project Site 530. In Hay, W. W., Sibuet, J.-C., et al., *Init. Repts. DSDP*, 75: Washington (U.S. Govt. Printing Office), 565-649.
- Thierstein, H. R., 1981. Late Cretaceous nannoplankton and the change at the Cretaceous-Tertiary boundary. In Warme, J., et al. (Eds.), *The Deep Sea Drilling Project: A Decade of progress* Soc. of Econ. Paleontol. Mineral. Spec. Pub. 32.
- van Heck, S. E., 1979a. Bibliography and taxa of calcareous nannoplankton. *It. Nannoplankton Assoc. Newsl.*, 1:AB1-5, A1-12, B1-27.
- \_\_\_\_\_, 1979b. Bibliography and taxa of calcareous nannoplankton. *Int. Nannoplankton Assoc. Newsl.*, 1:AB VI, A13-28, B28-42.
- \_\_\_\_\_, 1980a. Bibliography and taxa of calcareous nannoplankton. *Int. Nannoplankton Assoc. Newsl.*, 2:5-34.
- \_\_\_\_\_, 1980b. Bibliography and taxa of calcareous nannoplankton. *Int. Nannoplankton Assoc. Newsl.*, 2:43-81.
- \_\_\_\_\_, 1981a. Bibliography and taxa of calcareous nannoplankton. *Int. Nannoplankton Assoc. Newsl.*, 3:4-41.
- \_\_\_\_\_, 1981b. Bibliography and taxa of calcareous nannoplankton. *Int. Nannoplankton Assoc. Newsl.*, 3:51-86.
- \_\_\_\_\_, 1982a. Bibliography and taxa of calcareous nannoplankton. *Int. Nannoplankton Assoc. Newsl.*, 4:7-50.
- \_\_\_\_\_, 1982b. Bibliography and taxa of calcareous nannoplankton. *Int. Nannoplankton Assoc. Newsl.*, 4:65-96.
- \_\_\_\_\_, 1983. Bibliography and taxa of calcareous nannoplankton. *Int. Nannoplankton Assoc. Newsl.*, 5:4-13.
- Wind, F. H., 1979a. Late Campanian and Maestrichtian calcareous nannoplankton biogeography and high-latitude biostratigraphy [Ph.D. dissert.]. Florida State Univ., Tallahassee.
- \_\_\_\_\_, 1979b. Maestrichtian-Campanian nannoflora provinces of the southern Atlantic and Indian oceans. In Talwani, M., Hay, W. W., and Ryan, W.B.F. (Eds.), *Deep Sea Drilling Results in the Atlantic Ocean: Continental Margins and Paleoenvironment*. Am. Geophys. Union, Maurice Ewing Ser., 3:123-137.
- \_\_\_\_\_, 1983. The genus *Nephrolithus* Görka, 1957 (Coccolithophoridae). *J. Paleontol.*, 57:157-161.
- Wind, F. H., and Wise, S. W., 1978. Mesozoic holococcoliths. *Geology*, 6:140-142.
- \_\_\_\_\_, 1983. Correlation of upper Campanian-lower Maestrichtian calcareous nannofossil assemblages in drill and piston cores from the Falkland Plateau, southwest Atlantic Ocean. In Ludwig, W. J., Krasheninnikov, V. A., et al., *Init. Repts. DSDP*, 71: Washington (U.S. Govt. Printing Office), 551-563.
- Wise, S. W., 1983. Mesozoic and Cenozoic calcareous nannofossils recovered by Deep Sea Drilling Project Leg 71 in the Falkland Plateau region, southwest Atlantic Ocean. In Ludwig, W. J., Krasheninnikov, V. A., et al., *Init. Repts. DSDP*, 71: Washington (U.S. Govt. Printing Office), 481-550.
- \_\_\_\_\_, 1988. Mesozoic and Cenozoic history of calcareous nannofossils in the region of the Southern Ocean. *Palaeogeogr., Palaeoclimatol., Palaeoecol.*, 67:157-179.
- Wise, S. W., and Wind, F. H., 1977. Mesozoic and Cenozoic calcareous nannofossils recovered by DSDP Leg 36 drilling on the Falkland Plateau, Southwest Atlantic sector of the Southern Ocean. In Barker, P. F., Dalziel, I.W.D., et al., *Init. Repts. DSDP*, 36: Washington (U.S. Govt. Printing Office), 269-294.
- Worsley, T. R., 1974. The Cretaceous/Tertiary boundary event in the ocean. In Hay, W. W. (Ed.), *Studies in Paleo-oceanography*. Soc. of Econ. Paleontol. Mineral. Spec. Pub. 20.
- Worsley, T. R., and Martini, E., 1970. Late Maestrichtian nannoplankton provinces. *Nature*, 225:1242-1243.

Date of initial receipt: 27 February 1989  
 Date of acceptance: 18 September 1989  
 Ms 113B-124

## APPENDIX

Mesozoic Calcareous Nannofossils Considered in This Report  
in Alphabetical Order of Generic Epithets

- Acuturris scotus* (Risatti) Wind and Wise in Wise and Wind, 1977
- Ahmuelierella octoradiata* (Görka) Reinhardt, 1970
- Arkhangelskiella cymbiformis* Vekshina, 1959
- A. specillata* Vekshina, 1959
- Aspidolithus parvus constrictus* (Hattner et al.) Perch-Nielsen, 1984a
- Biantholithus sparsus* Bramlette and Martini, 1964
- Bidiscus rotatorius* Bukry, 1969
- Biscutum boletum* Wind and Wise in Wise and Wind, 1977
- B. castrorum* Black in Black and Barnes, 1959
- B. constans* (Görka) Black, 1959
- B. coronum* Wind and Wise in Wise and Wind, 1977
- B. dissimilis* Wind and Wise in Wise and Wind, 1977
- B. magnum* Wind and Wise in Wise and Wind, 1977
- B. notaculum* Wind and Wise in Wise and Wind, 1977
- Biscutum* sp.
- Boletuvelum candens* Wind and Wise in Wise and Wind, 1977
- Braarudosphaera* sp.
- Broinsonia enormis* (Shumenko) Manivit, 1971
- Broinsonia verecundia* Wind and Wise in Wise and Wind, 1977
- Centosphaera barbata* Wind and Wise in Wise and Wind, 1977
- Chiastozygus garrisonii* Bukry 1969
- Chiastozygus* sp.
- Corollithion rhombicum* (Stradner and Adamiker) Bukry, 1969
- Cretarhabdus conicus* Bramlette and Martini, 1964
- C. surrrellus* (Deflandre and Fert) Reinhardt emend. Thierstein, 1971
- Cribrosphaerella ehrenbergi* (Arkhangelsky) Deflandre in Piveteau, 1952
- C. daniae* Perch-Nielsen, 1973
- Cruciplacolithus* sp. cf. *C. inaeolus* Perch-Nielsen, 1969
- Cyclagelosphaera margerelii* Noel, 1965
- C. reinhardtii* (Perch-Nielsen) Romein, 1977
- Eiffellithus eximius* (Stover) Perch-Nielsen, 1968
- E. turrisseiffelii* (Deflandre in Deflandre and Fert) Reinhardt, 1965
- Gartnerago diversum* Thierstein, 1972
- Gartnerago* sp.
- Kamptnerius magnificus* Deflandre, 1959
- Lapideacassis mariae* Black emend. Wind and Wise in Wise and Wind, 1977
- L. tricornus* Wind and Wise in Wise and Wind, 1977
- Lapideacassis* sp.
- Lucianorhabdus arborius* Wind and Wise in Wise and Wind, 1977
- L. arcuatus* Forcheimer, 1972
- L. cayeuxii* Deflandre, 1959
- Markalius inversus* (Deflandre in Deflandre and Fert) Bramlette and Martini, 1964
- Markalius* sp.
- Marthasterites furcatus* (Deflandre in Deflandre and Fert) Deflandre, 1959
- Micula decussata* Vekshina, 1959
- Misceomarginatus pleniporus* Wind and Wise in Wise and Wind, 1977
- Monomarginatus pectinatus* Wind and Wise in Wise and Wind, 1977
- M. quaternarius* Wind and Wise in Wise and Wind, 1977
- Neocrepidolithus* Romein, 1979
- N. watkinsii* n. sp.
- Nephrolithus corystus* Wind, 1983
- N. frequens frequens* Görka, 1957
- N. f. miniporus* emend.
- Octocyclus magnus* Black, 1972
- Okkolithus australis* Wind and Wise in Wise and Wind, 1977
- Orastrum asarotum* Wind and Wise in Wise and Wind, 1977
- Phanulithus additus* Wind and Wise in Wise and Wind, 1977
- P. obscurus* (Deflandre) Wind and Wise in Wise and Wind, 1977
- P. ovalis* (Stradner) Wind and Wise in Wise and Wind, 1977
- Pharus simulacrum* Wind and Wise in Wise and Wind, 1977
- Prediscosphaera cretacea* (Arkhangelsky) Gartner, 1968
- P. spinosa* (Bramlette and Martini) Gartner, 1968
- P. stoveri* (Perch-Nielsen) Shafik and Stradner, 1971
- Psyktosphaera firthii* n. gen., n. sp.
- Reinhardtites* sp. aff. *R. anthophorus* (Deflandre) Perch-Nielsen, 1968

*R. levis* Prins and Sissingh, 1977

*Russelia multiplus* (Perch-Nielsen) Wind and Wise *in* Wise and Wind,  
1977

*Teichorhabdus ethmos* Wind and Wise *in* Wise and Wind, 1977

*Thoracosphaera* sp.

*Tranolithus phacelosus* Stover, 1966

*Vekshinella* sp.

*Watznaueria barnesae* (Black) Perch-Nielsen, 1968

*Zygodiscus compactus* Bukry, 1969

*Z. diplogrammus* (Deflandre and Fert) Gartner, 1968

*Z. sigmoides* Bramlette and Sullivan, 1961

*Z. spiralis* Bramlette and Martini, 1964

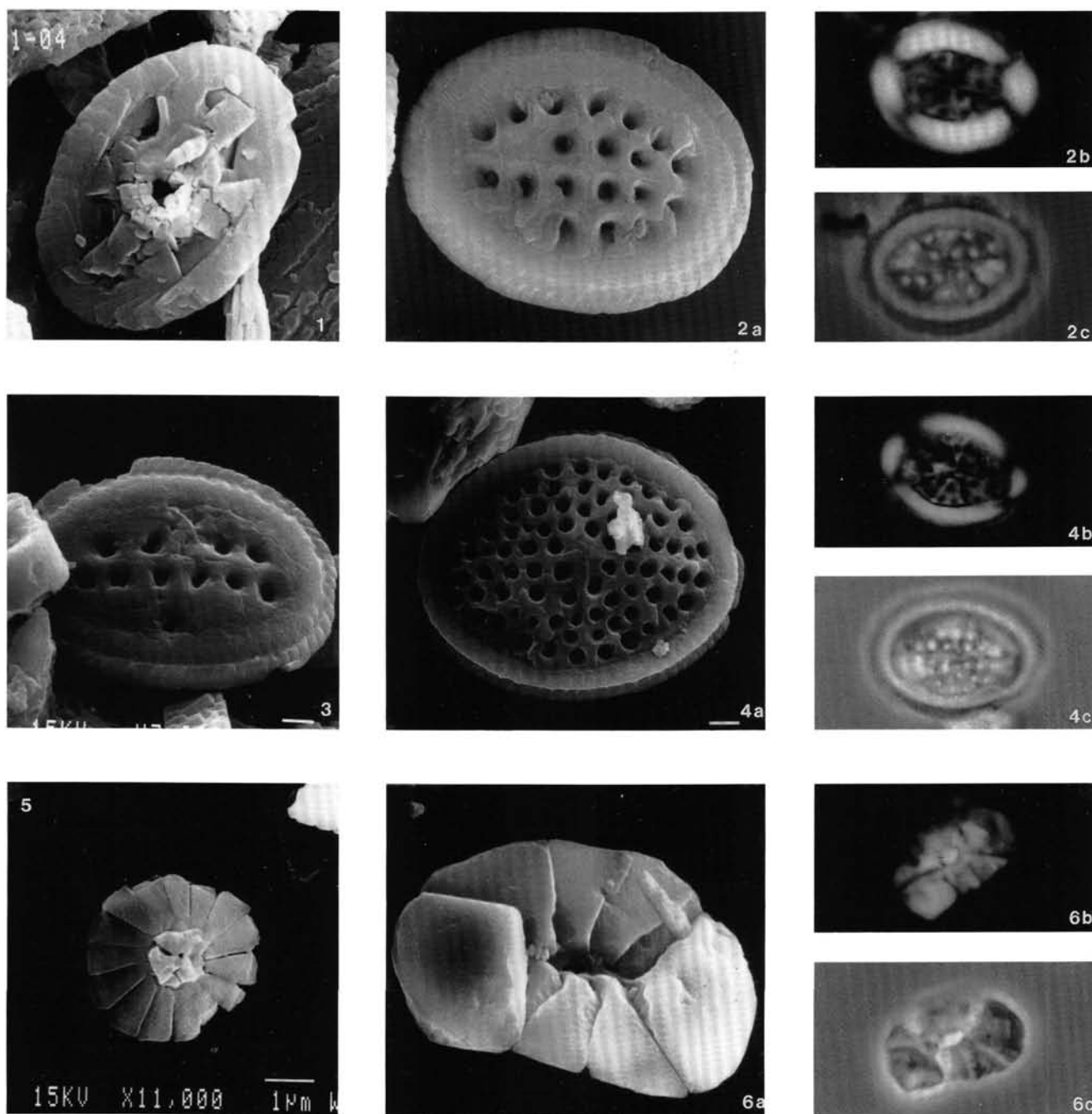


Plate 1. Note on the plates: All micrographs of coccoliths are of the distal view except where noted otherwise. Pol., Ph., Tr., and SEM denote polarized, phase contrast, transmitted, and scanning electron micrographs, respectively. Where more than one illustration is provided of a specimen, the sample and magnification designation are not repeated in the caption. 1. *Ahmuellerella octoradiata*, Sample 113-690C-20X-2, 28–30 cm, SEM,  $\times 7000$ . 2a–c. *Arkhangelskiella cymbiformis*, Sample 113-690C-19X-2, 130–132 cm. (a) SEM,  $\times 5500$ ; (b) Pol,  $\times 2300$ ; (c) Ph. 3. *Aspidolithus* sp. cf. *A. parvus parvus*, Sample 113-690C-20X-2, 29–31 cm, SEM,  $\times 5000$ . 4a–c. *Arkhangelskiella specillata*, (a) Section 113-690C-20X, CC, SEM,  $\times 5000$ ; (b) Sample 113-690C-19X-4, 130–132 cm, Pol,  $\times 1700$ ; (c) Ph. 5. *Bidiscus rotatorius*, Sample 113-690C-19X-2, 130–132 cm, SEM,  $\times 7000$ . 6a–c. *Biscutum dissimilis*, (a) Sample 113-690C-19X-2, 130–132 cm, SEM,  $\times 6500$ ; (b) Sample 113-690C-19X-4, 130–132 cm, Pol,  $\times 2100$ ; (c) Ph.

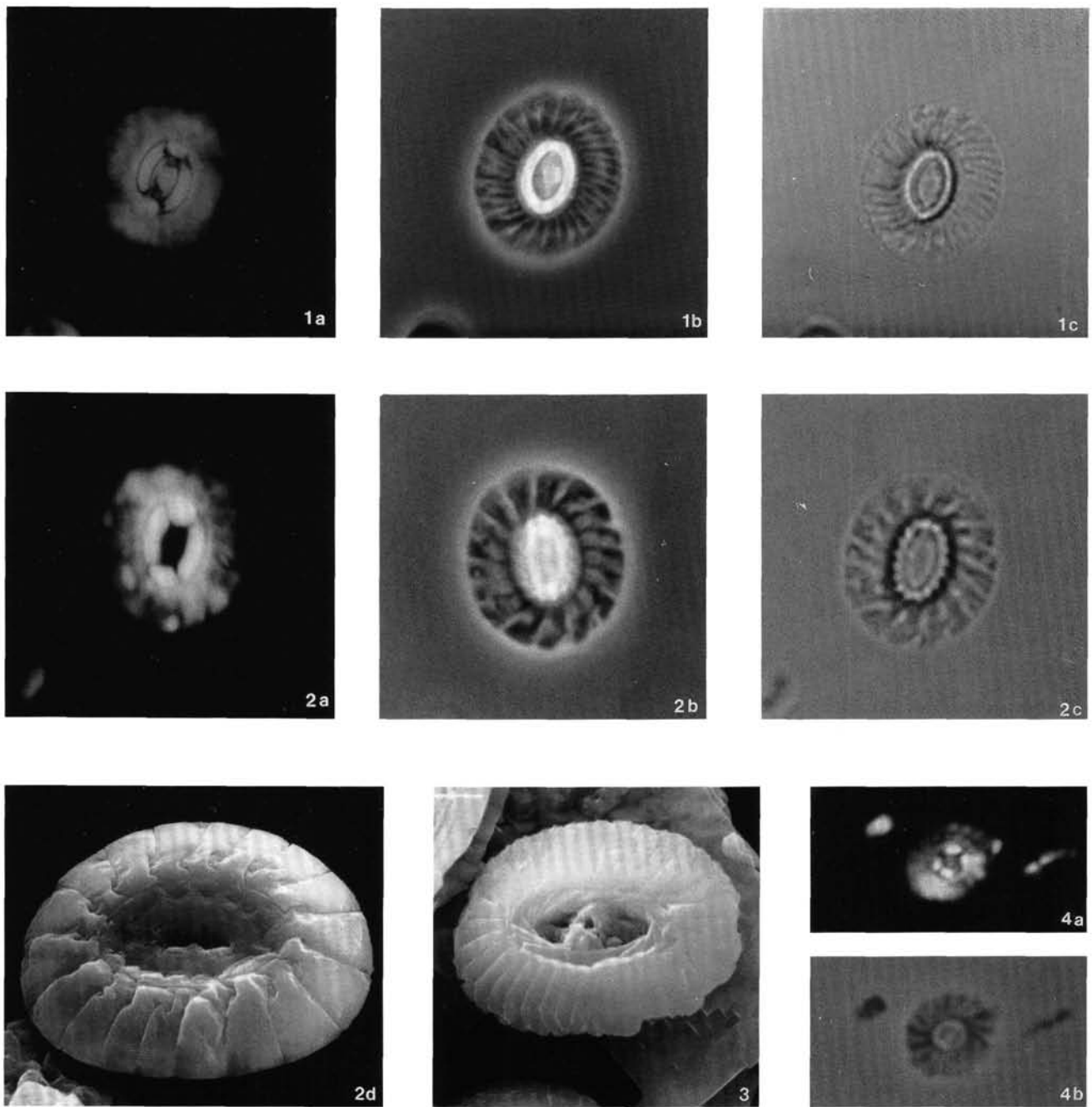


Plate 2. **1a-c.** *Biscutum coronum*, Sample 113-690C-20X-2, 28-30 cm. (a) Pol,  $\times 2000$ ; (b) Ph; (c) Tr. **2a-d.** *Biscutum magnum*, (a) Sample 113-690C-20X-2, 28-30 cm, Pol,  $\times 2800$ ; (b) Ph; (c) Tr; (d) Sample 113-690C-19X-2, 130-132 cm, SEM,  $\times 6000$ . **3.** *Biscutum notaculum*, Section 113-690C-20X, CC, SEM,  $\times 8000$ . **4a-b.** *Biscutum constans*, Sample 113-690C-19X-4, 130-132 cm. (a) Pol,  $\times 3500$ ; (b) Ph.

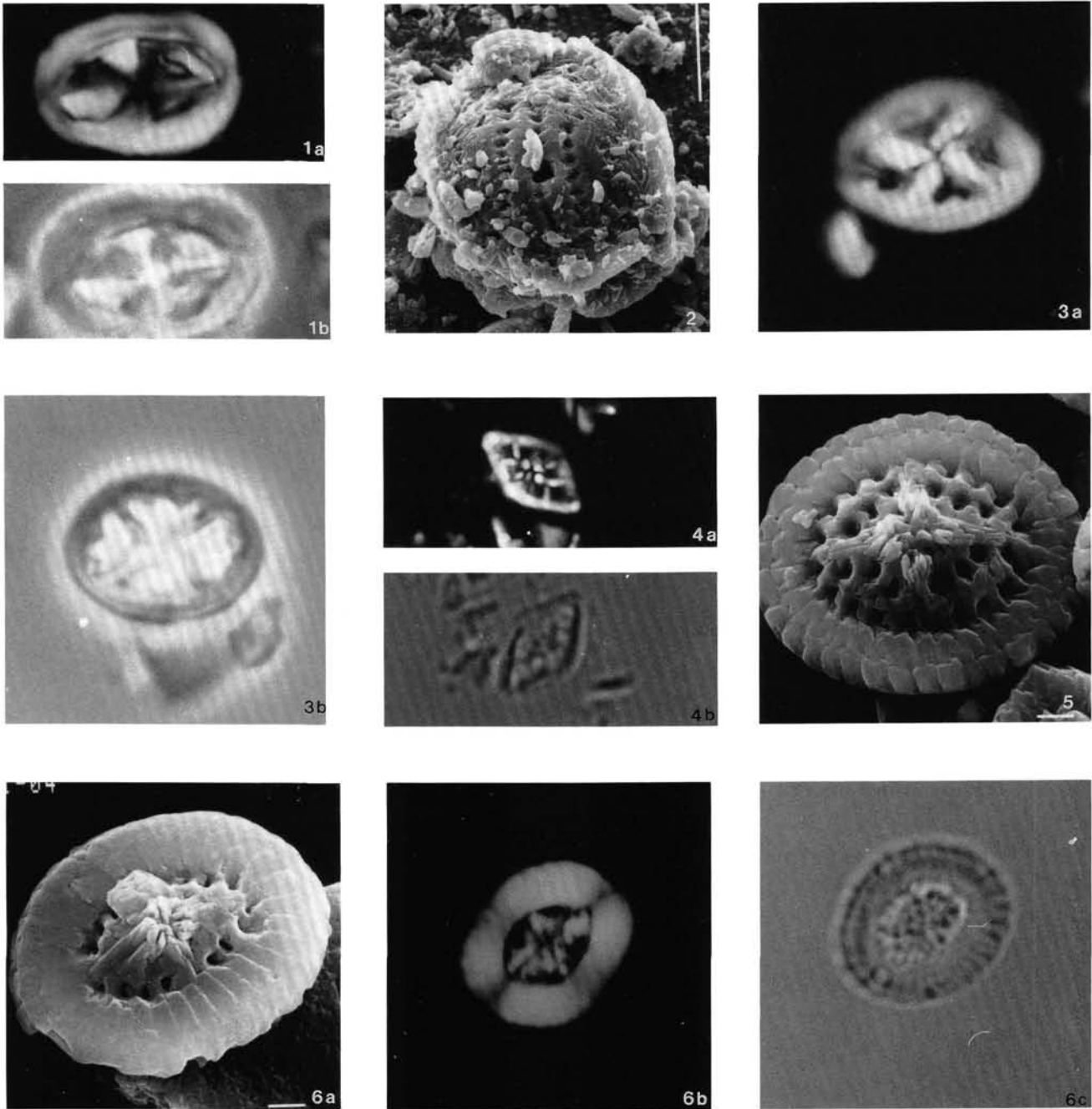


Plate 3. **1a-b.** *Broinsonia enormis*, Sample 113-690C-22X-2, 133-135 cm. (a) Pol,  $\times 2900$ ; (b) Ph. **2.** *Centosphaera barbata*, Sample 113-690C-19X-4, 130-132 cm, SEM,  $\times 1000$ . **3a-b.** *Chiastozygus garrisonii*, Sample 113-690C-19X-3, 130-132 cm; (a) Pol,  $\times 6700$ ; (b) Ph. **4a-b.** *Corolithion rhombicum*, Sample 113-690C-20X-1, 30-32 cm. (a) Pol,  $\times 3600$ ; (b) Tr. **5.** *Cretarhabdus conicus*, Sample 113-690C-19X-2, 130-132 cm, SEM,  $\times 6000$ . **6a-c.** *Cretarhabdus surirellus*, (a) Sample 113-690C-19X-2, 130-132 cm, SEM,  $\times 6000$ ; (b) Sample 113-690C-20X-2, 28-30 cm, Pol,  $\times 2700$ ; (c) Tr.

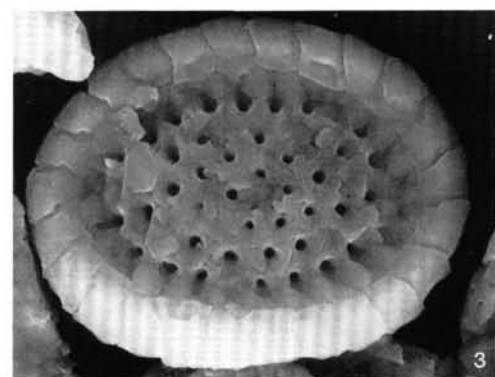
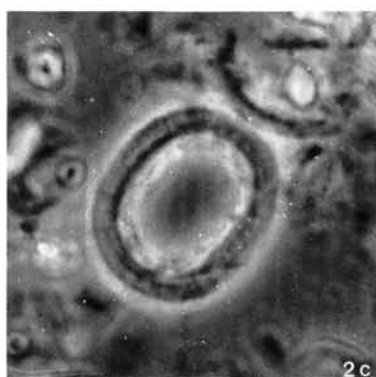
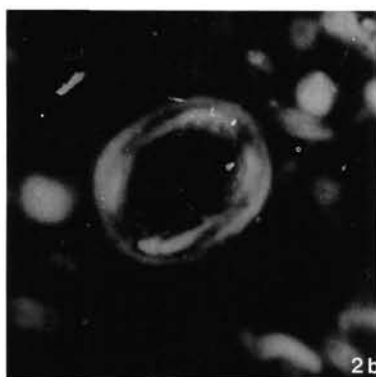
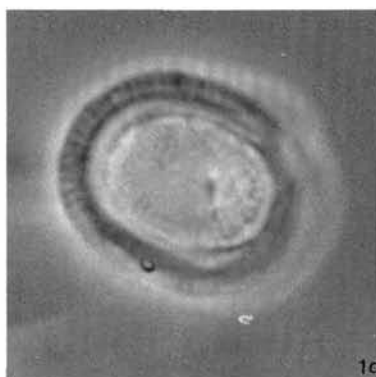
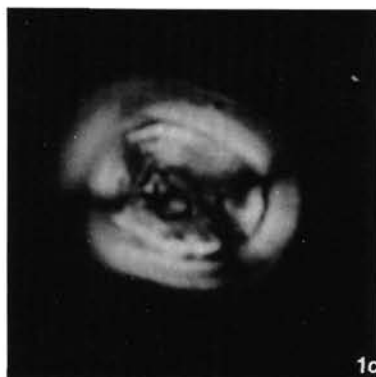
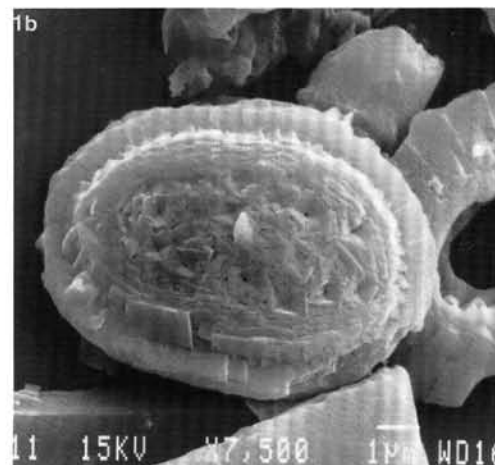
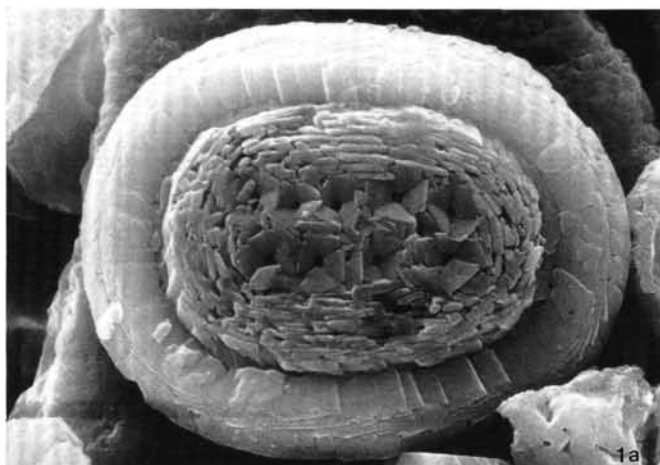


Plate 4. **1a-d.** *Psyktoisphaera firthii*, (a) Holotype, Sample 113-690C-19X-2, 130-132 cm, SEM,  $\times 7500$ ; (b) Isotype, Sample 113-690C-21X-3, 28-30 cm, SEM,  $\times 5500$ ; (c) Sample 113-690C-19X-2, 130-132 cm, Pol,  $\times 3100$ ; (d) Tr. **2a-c.** *Cribrosphaerella daniae* (rim), (a) Sample 113-690C-18X-3, 28-30 cm, SEM,  $\times 5700$ ; (b) Sample 113-690C-15X-4, 43-44 cm, Pol,  $\times 1750$ ; (c) Ph. **3.** *Cribrosphaerella ehrenbergii*, Sample 113-690C-19X-2, 130-132 cm, SEM,  $\times 6600$ .

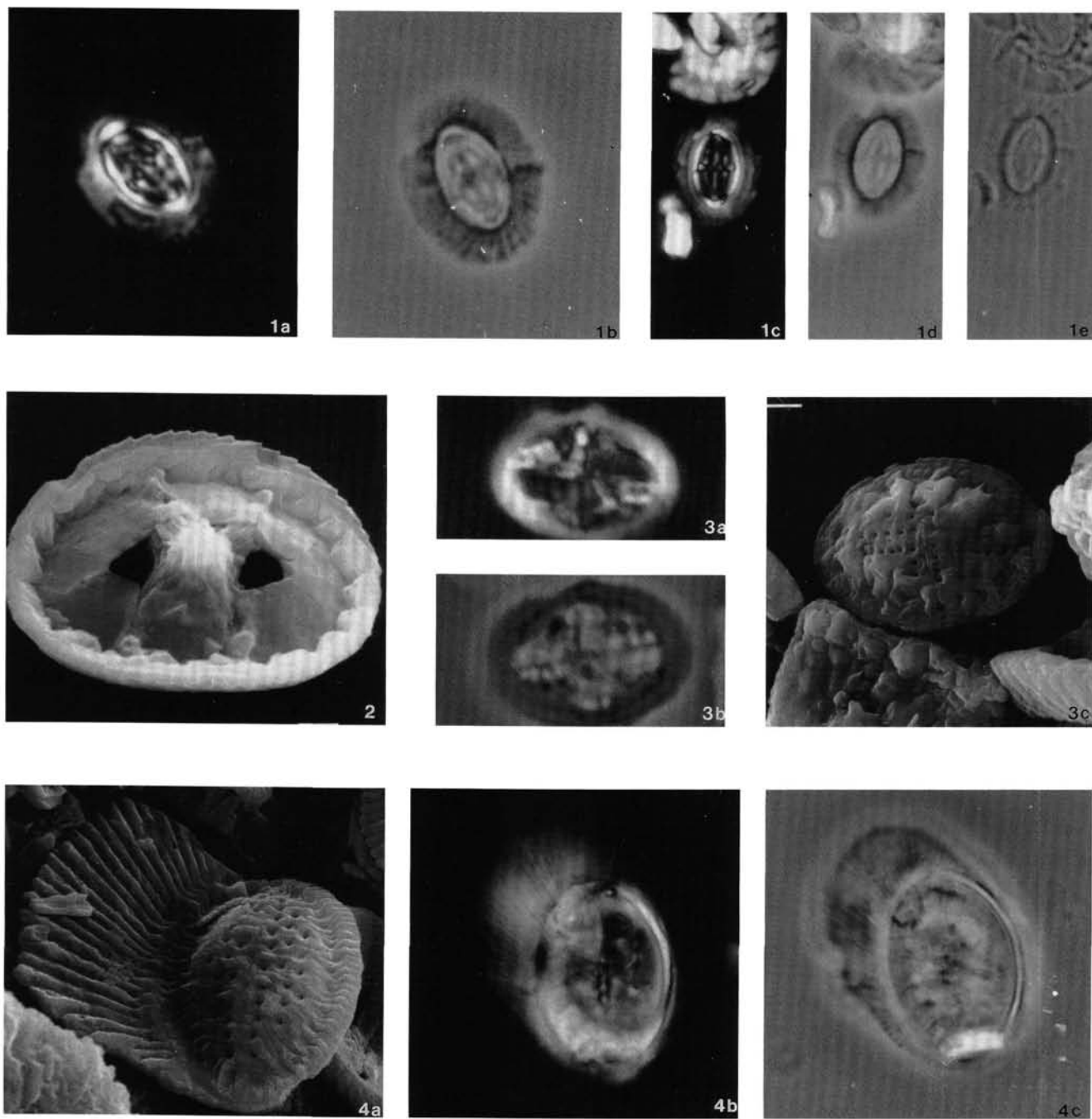


Plate 5. **1a-e.** *Cruciplacolithus* sp. cf. *C. inaeolus*, (a) Sample 113-690C-19X-4, 130-132 cm, Pol,  $\times 2700$ ; (b) Ph; (c) Sample 113-690C-19X-4, 130-132 cm, Pol,  $\times 2300$ ; (d) Ph; (e) Tr. **2.** *Eiffellithus turriseiffelii*, Sample 113-690C-20X-2, 28-30 cm, SEM,  $\times 6500$ . **3a-c.** *Gartnerago diversum*, (a) Sample 113-690C-19X-3, 130-132 cm, Pol,  $\times 3400$ ; (b) Ph; (c) Sample 113-690C-20X-2, 28-30 cm, SEM,  $\times 6000$ . **4a-c.** *Kamptnerius magnificus*, (a) Sample 113-690C-21X-3, 28-30 cm, SEM,  $\times 4500$ ; (b) Sample 113-690C-19X-4, 130-132 cm, Pol,  $\times 2000$ . (c) Ph.

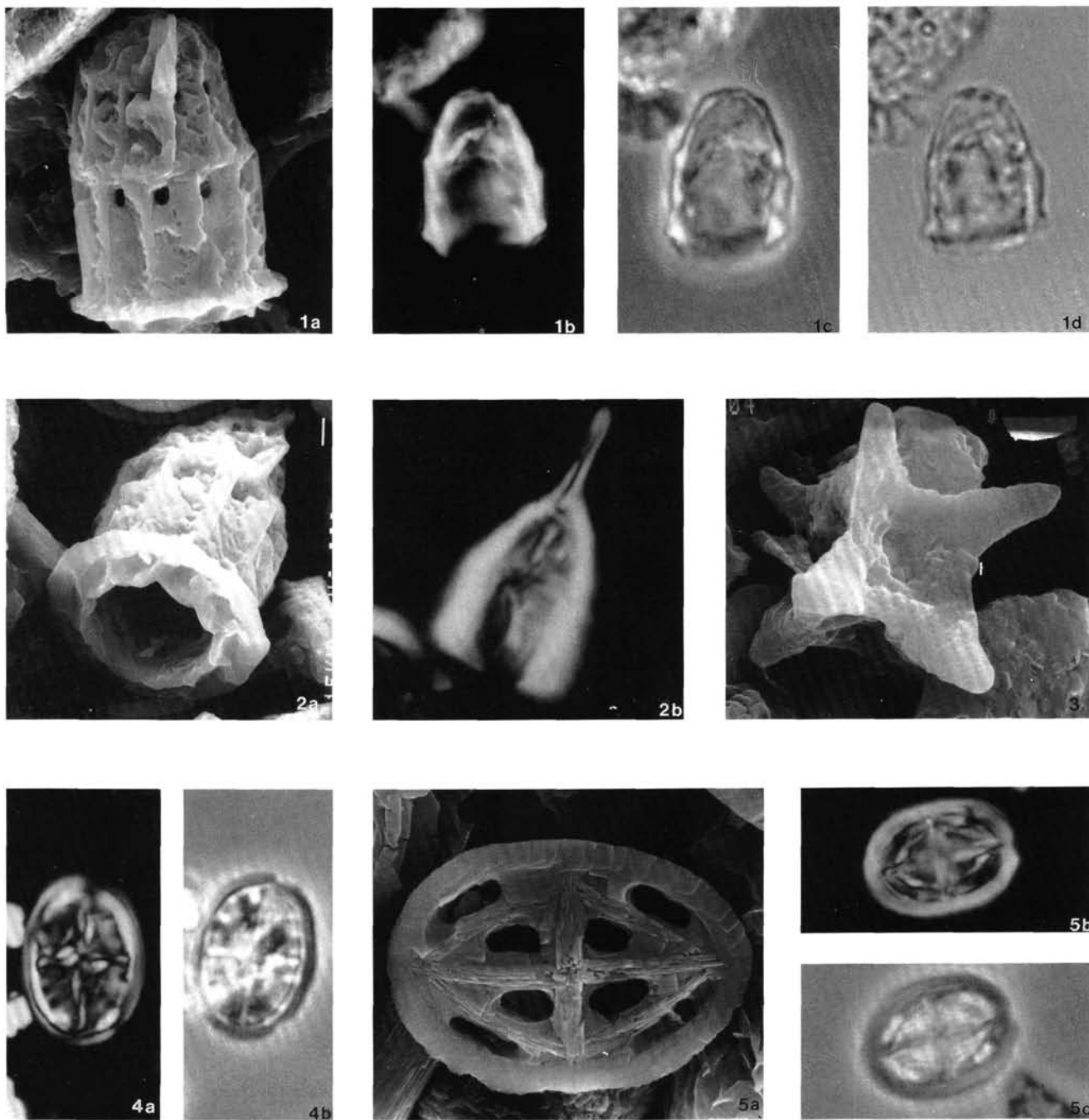


Plate 6. **1a-d.** *Lapideacassis tricornus*, (a) Sample 113-690C-20X-1, 133-135 cm, SEM,  $\times 4500$ ; (b) Sample 113-690C-20X-1, 30-32 cm, Pol,  $\times 2100$ ; (c) Ph; (d) Tr. **2a-b.** *Lapideacassis mariae*, (a) Sample 113-690C-20X-1, 133-135 cm, SEM,  $\times 4500$ ; (b) Sample 113-690C-19X-3, 130-132 cm, Pol,  $\times 3300$ . **3.** *Micula decussata*, Sample 113-690C-21X-4, 8-10 cm, SEM,  $\times 7500$ . **4a-b.** *Misceomarginatus pleniporus*, Sample 113-690C-22X-2, 133-135 cm (a) Pol,  $\times 2600$ ; (b) Ph. **5a-c.** *Monomarginatus quaternarius*, (a) Sample 113-690C-20X-2, 133-135 cm, SEM,  $\times 6200$ ; (b) Sample 113-690C-19X-3, 130-132 cm, Pol,  $\times 2600$ ; (c) Ph.

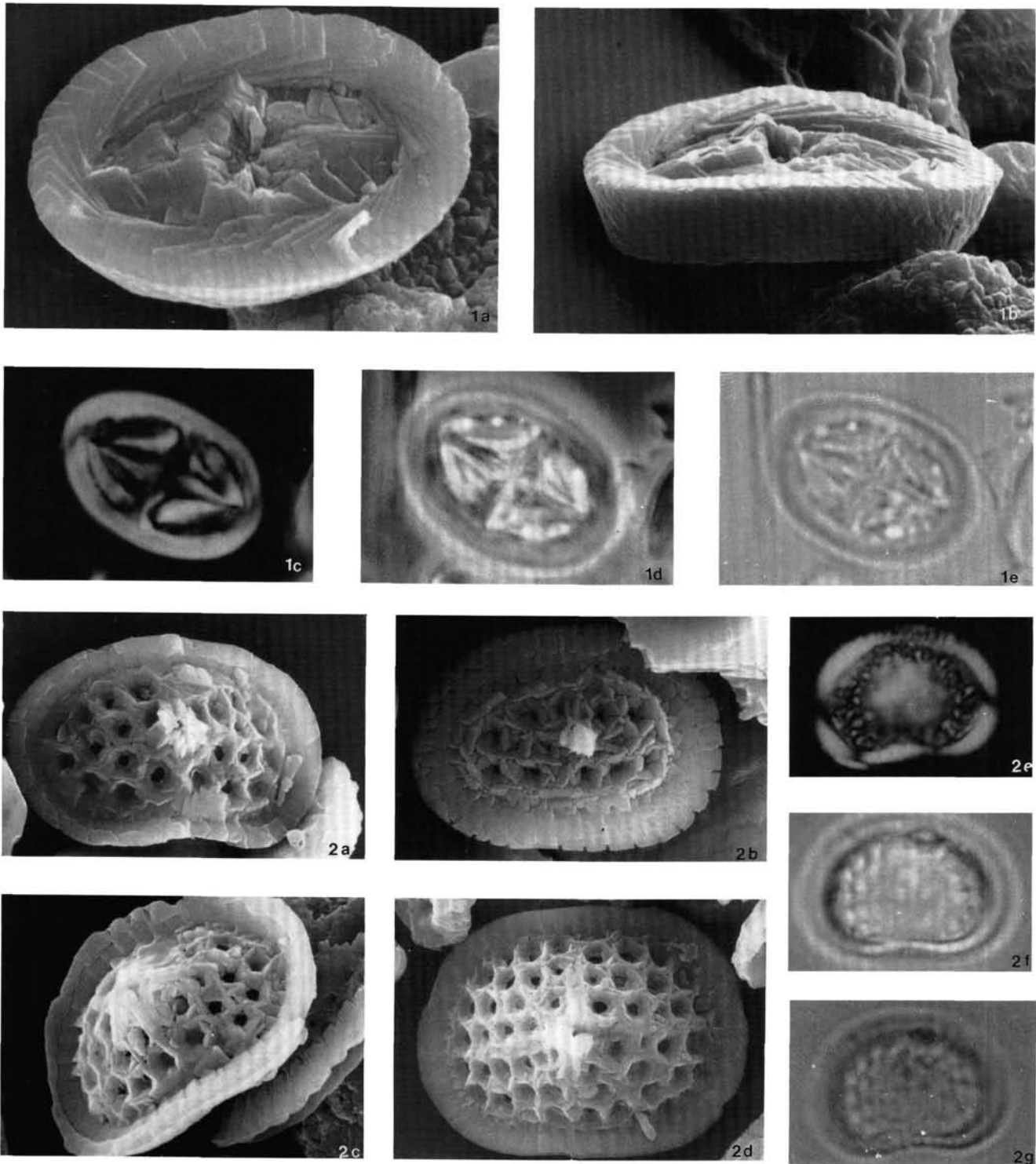


Plate 7. **1a-e.** *Neocrepidolithus watkinsii* n. sp., (a) Holotype, Sample 113-690C-21X-3, 28-30 cm, SEM,  $\times 7500$ ; (b) side view of specimen (a); (c) Isotype, Sample 113-690C-20X-2, 28-30 cm, Pol,  $\times 3000$ ; (d) Ph; (e) Tr. **2a-g.** *Nephrolithus corystus*, (a) Sample 113-690C-19X-2, 130-132 cm, SEM,  $\times 5500$ ; (b) Sample 113-690C-20X-1, 133-135 cm, SEM,  $\times 8000$ ; (c) Sample 113-690C-21X-4, 8-10 cm, SEM,  $\times 7500$ ; (d) Sample 113-690C-19X-2, 130-132 cm, SEM,  $\times 5500$ ; (e) Sample 113-690C-19X-4, 130-132 cm, Pol,  $\times 3100$ ; (f) Ph; (g) Tr.

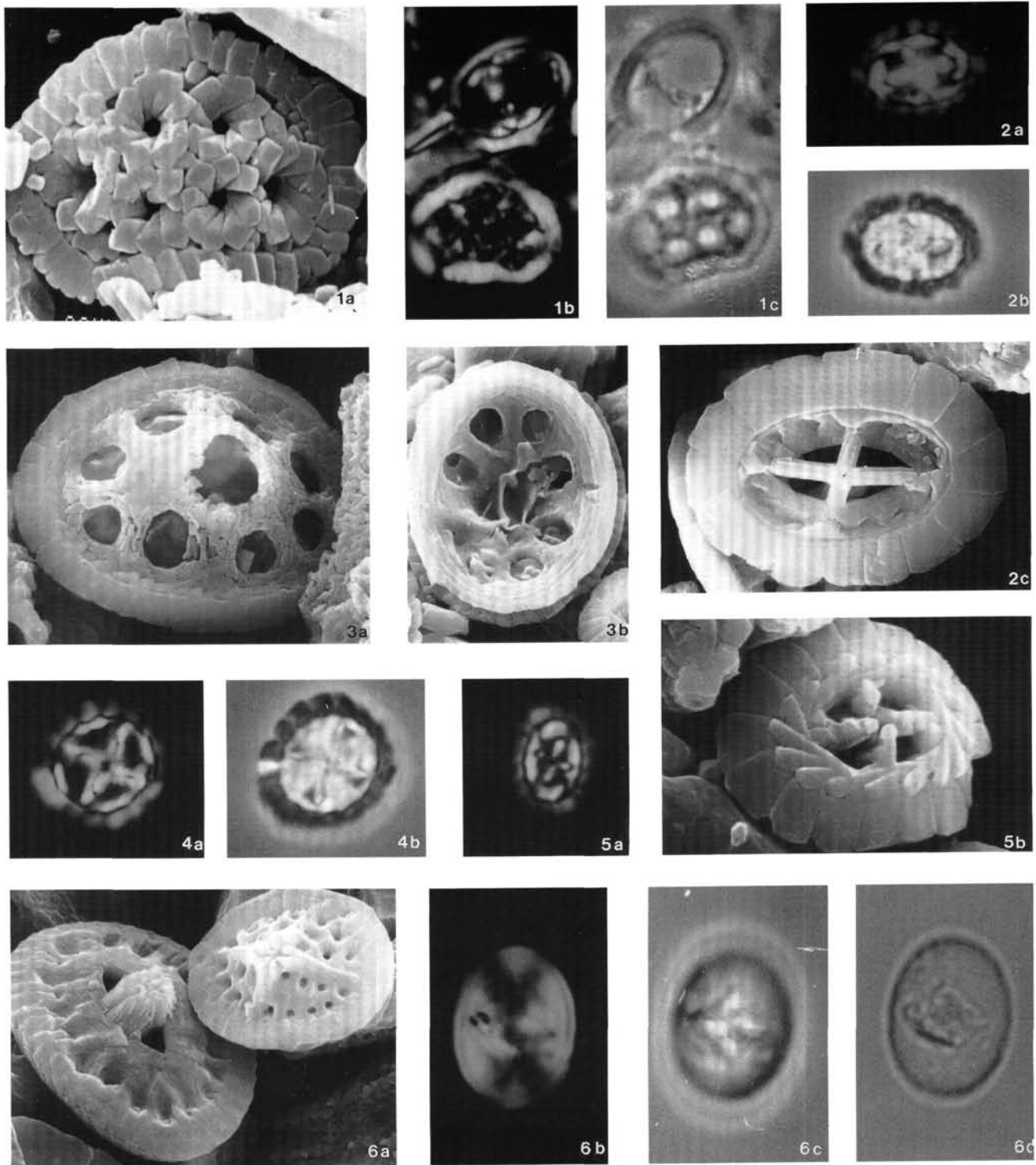


Plate 8. **1a-c.** *Nephrolithus frequens*, (a) Sample 113-690C-15X-4, 66-67 cm, SEM,  $\times 7750$ ; (b) *N. frequens* and *Zygodiscus sigmoides*, Sample 113-690C-15X-4, 43-44 cm, Pol,  $\times 2600$ ; (c) Ph. **2a-c.** *Prediscosphaera spinosa*, (a) Sample 113-690C-22X-2, 133-135 cm, Pol,  $\times 3000$ ; (b) Ph; (c) Sample 113-690C-19X-2, 130-132 cm, SEM,  $\times 6000$ . **3a-b.** *Octocyclus magnus*, Sample 113-690C-20X-1, 133-135 cm; (a) SEM,  $\times 7000$ ; (b) SEM,  $\times 4900$ , proximal view. **4a-b.** *Prediscosphaera cretacea*, Sample 113-690C-22X-2, 133-135 cm (a) Pol,  $\times 2300$ ; (b) Ph. **5a-b.** *Prediscosphaera stoveri*, (a) Sample 113-690C-19X-4, 130-132 cm, Pol,  $\times 2800$ ; (b) Section 113-690C-18X, CC, SEM,  $\times 11,000$ . **6a.** *Reinhardtites* sp. aff. *R. anthophorus* (left) with *Cretarhabdus conicus*, Sample 113-690C-21X-4, 8-10 cm, SEM,  $\times 6000$ ; **6b-d.** *R.* sp. aff. *R. anthophorus*, Sample 113-690C-21X-2, 28-30 cm; (b) Pol,  $\times 2300$ ; (c) Ph; (d) Tr.

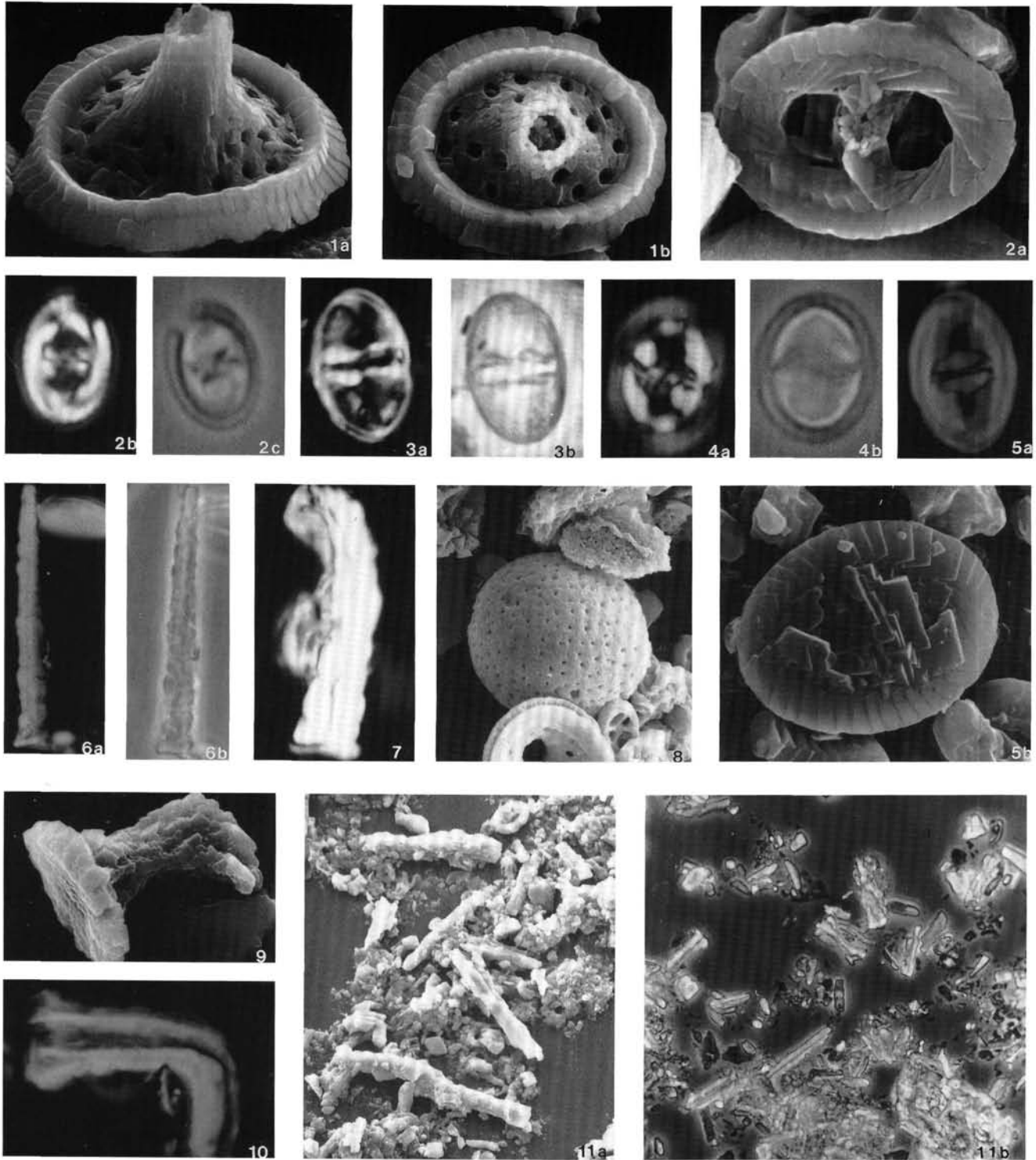


Plate 9. **1a-b.** *Teichorhabdus ethmos*, (a) Sample 113-690C-20X-2, 28–30 cm, SEM,  $\times 4800$ ; (b) Sample 113-690C-19X-2, 130–132 cm, SEM,  $\times 4000$ . **2a-c.** *Zygodiscus spiralis*, Sample 113-690C-19X-2, 130–132 cm. (a) SEM,  $\times 9500$ ; (b) Pol,  $\times 4800$ ; (c) Ph. **3a-b.** *Zygodiscus diplogrammus*, Sample 113-690C-20X-2, 28–30 cm. (a) Pol,  $\times 2400$ ; (b) Ph. **4a-b.** *Zygodiscus sigmoides*, Sample 113-690C-19X-3, 130–132 cm. (a) Pol,  $\times 2600$ ; (b) Ph. **5a-b.** *Zygodiscus compactus*, (a) Sample 113-690C-19X-3, 130–132 cm, Pol,  $\times 2900$ ; (b) Sample 113-690C-19X-4, 130–132 cm, SEM,  $\times 6200$ . **6a-b.** *Acuturris scotus*, Sample 113-690C-19X-3, 130–132 cm. (a) Pol,  $\times 1500$ ; (b) Ph. **7.** *Lucianorhabdus cayeuxii*, Section 113-690C-20X, CC, Pol,  $\times 2300$ . **8.** *Thoracosphaera* sp., Sample 113-690C-21X-3, 28–30 cm, SEM,  $\times 2100$ . **9.** *Lucianorhabdus arborius*, Sample 113-690C-19X-2, 130–132 cm, SEM,  $\times 3500$ . **10.** *Lucianorhabdus arcuatus*, Sample 113-690C-19X-4, 130–132 cm, Pol,  $\times 2700$ . **11a-b.** Holococcoliths, Sample 113-690C-22X-5, 29–31 cm. (a) SEM,  $\times 850$ ; (b) Ph,  $\times 340$ .